

Maryland Department of Natural Resources  
Resource Assessment Service  
MARYLAND GEOLOGICAL SURVEY  
Richard A. Ortt, Jr., Director

Report of Investigations No. 83

CONTRIBUTIONS OF SHORE EROSION AND  
RESUSPENSION TO NEARSHORE TURBIDITY IN THE  
CHOPTANK RIVER, MARYLAND

by

Jeffrey P. Halka  
and  
Lawrence P. Sanford



Prepared in cooperation with the  
University of Maryland, Center for Environmental Science

DNR Publication No. 12-632013-650  
UMCES Contribution No. 4769

2014

# CONTENTS

	<b>Page</b>
INTRODUCTION .....	1
SITE CHARACTERIZATION.....	2
METHODS .....	6
Geomorphic and Geological Studies.....	6
Historical Shoreline Mapping and Erosion Rate Estimation .....	9
Nearshore Resuspension Measurements .....	12
Settling Velocity Experiments .....	15
Exploratory Modeling .....	16
RESULTS .....	21
Geomorphic and Geological Studies.....	21
Historical Shoreline Mapping and Erosion Rate Estimation .....	31
Nearshore Resuspension Measurements .....	38
Settling Velocity Experiments .....	47
Exploratory Modeling .....	50
ACKNOWLEDGEMENTS.....	54
REFERENCES .....	55
APPENDIX.....	57

## FIGURES

Figure	Page
1. Location of the intensive study area on the south shore of the Choptank River .....	2
2. Aerial photo of the Todds Point peninsula .....	3
3. View toward the northeast and to the southwest at the Todds Point peninsula.....	4
4. Contoured 2003 LIDAR data of the Todds Point intensive study area .....	5
5. Comparative plot of the Cambridge Tide Station water levels with the Todd Point Tide Station water level.....	7
6. Historical shorelines in the Todds Point area .....	10
7. Schematic of SWATT bottom tripod.....	13
8. CTD with OBS-3 turbidity sensor attached to kayak and kayak survey underway.....	15
9. 1 cubic meter mesocosm used for settling velocity experiments.....	15
10. Plot of the structure function $f(x)$ in Equation 13 .....	19
11. Location of bank samples collected in the Choptank River estuary .....	22
12. Eroding bank face on the north shore of Todds Point East Station .....	24
13. Eroding bank at Todds Point fronted by a wedge of beach sand with exposed Kent Island Formation sediments.....	25
14. Exposed eroding Pleistocene Kent Island Formation .....	25
15. Nearshore low amplitude sand bars exposed at Todds Point.....	26
16. Bathymetry offshore of Todds Point intensive study area.....	28
17. Offshore depth profiles along the three shore normal transects.....	29
18. Measured shore erosion over a one-year period at Todds Point.....	30
19. Representation of the fastland and nearshore components of shore erosion .....	31
20. Reaches in the Choptank river for which shore erosion rates were calculated.....	33
21. Unprotected profiles 1 and 2 at the Todds Point study area .....	37
22. Bathymetric map offshore of Todds Point with locations of moored sensors.....	38
23. Time series from moored sensors for the period of the 2002 deployment .....	39
24. Time series from moored sensors for the period of the 2003 deployment .....	40
25. Time series from moored sensors from October 29 – November 1, 2002.....	42
26. Interpolated map of TSS from the boat survey late on Oct. 31, 2002 .....	43
27. Time series from moored sensors from Nov 6 – 9, 2002.....	44
28. Interpolated maps of TSS from boat surveys of November 8 and 21, 2002.....	45
29. Time series from moored sensors from Nov 13-16, 2003 .....	46
30. Interpolated map of TSS from the boat survey of November 21, 2003.....	47
31. Time series of mass concentration, volume concentration, mass concentration with exponential decay fits, and median suspended particle diameter .....	48
32. LISST size distributions from field observations and laboratory observations.....	49
33. Initial concentration vs. derived settling speed from the laboratory experiments .....	50
34. Bathymetry along cross-sections off the unprotected and protected shorelines compared to the equilibrium 2/3 power law model .....	51
35. Time series of lowpass filtered model-predicted wave height, observed tidal height and predicted shoreline retreat from Model A and Model B.....	52
36. Observed nearshore TSS time series from the unprotected side sensor, predicted shoreline erosion impulse from Model A and predicted shoreline erosion impulse from Model B .....	53

## TABLES

<b>Table</b>	<b>Page</b>
1. Sources of Historical Shorelines, Choptank River .....	11
2. Locations and times for resuspension studies .....	12
3. Bulk properties and sediment composition for shore samples.....	23
4. Bank sediment characteristics at the Todds Point Intensive Study area.....	27
5. Total shoreline length and protected length for individual reaches .....	34
6. Volume and mass of sediment delivered from shore erosion for individual reaches .....	35
7. Summary statistics from all deployed turbidity sensors .....	41
8. Summary of results of laboratory settling experiments .....	48

## INTRODUCTION

Suspended sediments are considered to have potentially significant ecosystem consequences in the Chesapeake Bay which include:

- Contributing to light attenuation, thus inhibiting the growth of submersed aquatic vegetation
- Interfering with the functionality of filter feeding organisms, both pelagic and benthic
- Potential burial of sessile benthic organisms

While the consequences of water column turbidity are broadly understood, the sources and spatial and temporal variations of shallow water turbidity are poorly documented and only generally known. Suspended sediments in the water column can arise from local resuspension, advection from nearby sources, erosion of the adjacent shore, and upstream watershed sources. The contribution of suspended sediment to light attenuation in comparison to the attenuation from dissolved materials and planktonic organisms also is not well documented in shallow waters of the Chesapeake Bay.

This project addressed the specific contributions of shore erosion and nearshore resuspension to nearshore turbidity. The work was performed in a tributary system of the Chesapeake Bay, the Choptank River. This tributary exhibits a range of geomorphic characteristics that are common to many of the other tributaries of the Bay as well as the mainstem Bay itself: 1) a broad embayed mouth region where the fetch is large, the water is deep and many reaches of the shore are very exposed; 2) a narrower brackish tidal reach where fetch is more restricted but tidal velocities are enhanced; and, 3) a progressively narrowing upstream portion where fluvial influences are more dominant. The work focused specifically on an exposed headland in the mouth region where rapid shore erosion is an ongoing problem, Todds Point.

This study comprised was comprised of four components to determine the sources of nearshore suspended sediments, including:

- 1) a mapping based estimate of the long-term contribution of shore erosion as a nearshore suspended particulate source,
- 2) a field oriented process study relating wind generated wave forcing and tidal forcing to resuspended sediment concentrations,
- 3) settling experiments to determine the rate at which particles are removed from suspension by settling under various levels of turbulence, and
- 4) a preliminary modeling effort relating wind and tidal forcing to shore erosion rates.

This work contributed to the *Chesapeake 2000* agreement's commitment to reduce Chesapeake Bay sediment loads to support the aquatic living resources of the Bay and its tributaries and to remove these waters from the list of impaired waters under the Clean Water Act by 2010 ([http://www.chesapeakebay.net/content/publications/cbp\\_12081.pdf](http://www.chesapeakebay.net/content/publications/cbp_12081.pdf)). The study provides a basis for setting achievable sediment reduction goals under the Clean Water Act through increasing the understanding of sediment loads attributable to shore erosion.

## SITE CHARACTERIZATION

Todds Point, the location of the intensive study area, is a flat lying peninsula with a low elevation and is mostly in farm field. Farming takes place nearly to the edge of the banks facing the water. Location of the peninsula on the south shore of the Choptank River near the mouth is shown in Figure 1. The site is exposed to significant fetch from the northwest, north, and northeast where distances to opposite shorelines exceed 10 kilometers. To the west-northwest, through the open mouth of the Choptank River, the distance to the western shore of the Bay is over 20 kilometers. However, incident waves from this direction are probably attenuated somewhat by the presence of Sharps Island Shoal at the Choptank River mouth, and by Cooks Point located immediately to the west of Todds Point. In the past, Cooks Point undoubtedly provided more protection to Todds Point from westerly approaching waves than at the present, due to the fact that the narrow Cooks Point peninsula has been eroding rapidly (Maryland Geological Survey 2000, 2001).

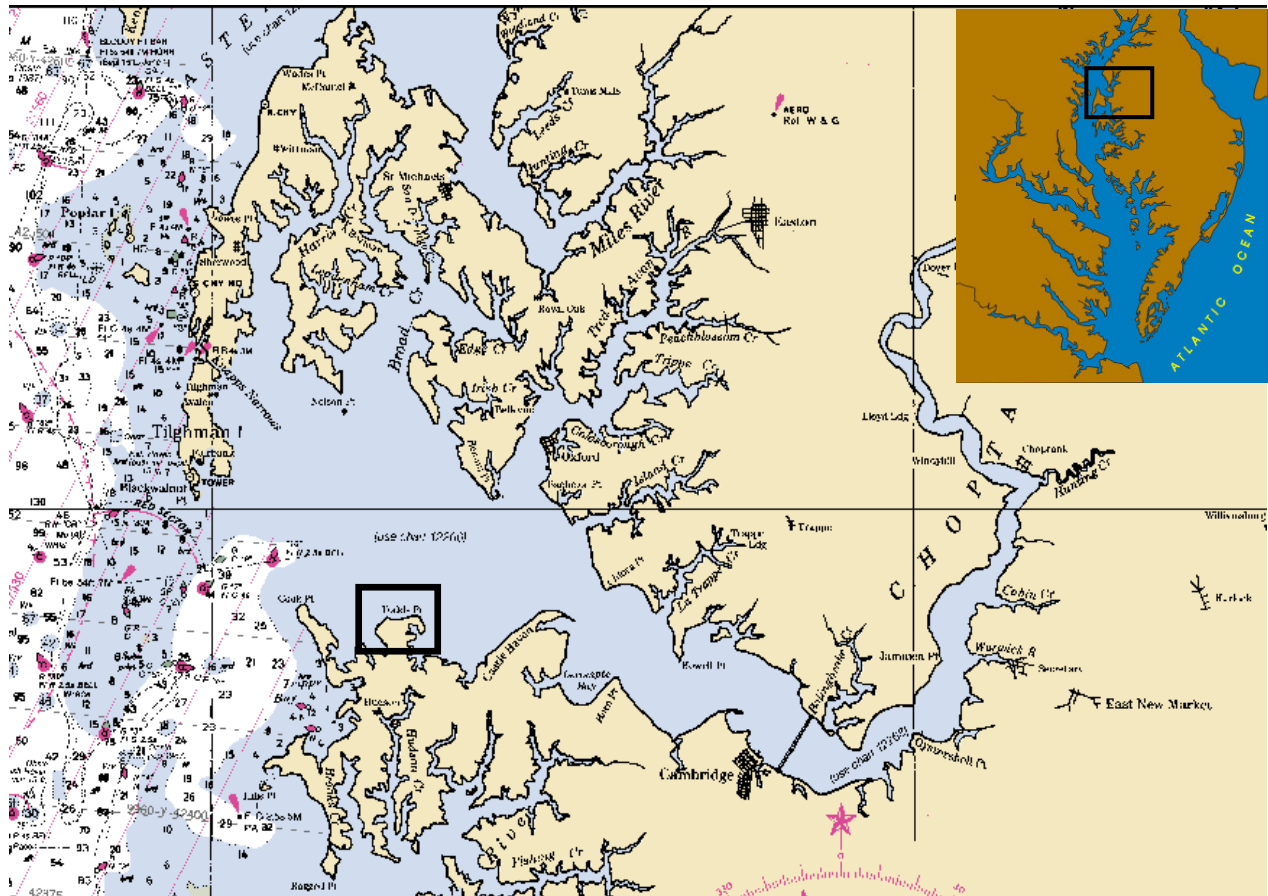


**Figure 1. Location of the intensive study area on the south shore of the Choptank River at Todds Point indicated by the box, which is shown in more detail in Figure 2. Note the Cook Point peninsula located immediately to the west.**

The location of the intensive study area on the peninsula is indicated by the arrow in Figure 2. The shore to the northeast of the arrowhead is unprotected, while the shore to the southwest is protected by a revetment. It is readily apparent that the northeast section of shore has eroded substantially relative to the protected section of shore to the southwest. The revetment was emplaced in 1977 (Robert Spedden, property owner, personal communication). Extensive farm fields occupy most of the peninsular area as seen on the air photo. Shore parallel sand bars are also notable along most of the northward facing portion of the shore.

The sharp contrast between protected and unprotected shorelines directly adjacent to each other, both exposed to significant wind fetch from the NW, was the primary reason for selecting this site for intensive study. The fact that a major hurricane flooding event (Hurricane Isabel, September 2003) occurred during the year immediately following the initial survey during the fall of 2002 led to the decision to reoccupy the same site in the second year of the study.



**Figure 2 Aerial photo of the Todds Point peninsula showing the location of the intensive study area at the arrow.**

Figure 3 shows views along both the unprotected shoreline looking toward the northeast and the protected shoreline looking towards the southwest. Along the unprotected shoreline (Figure 3, left), the characteristics of the low bank are evident as is the farm field behind the eroding shore. Also notable is the lack of significant sand or a beach fronting the eroding shore, due to the fact that the eroding bank sediments are composed predominantly of fine grained silts and clays. The shoreline to the southwest is protected by a continuous revetment (Figure 3, right). The extent of wave run-up on the stone revetment is apparent from the darker stained stones.



**Figure 3 Left - View toward the northeast along the unprotected portion of the Todds Point peninsula. Note the differential erosion of the bank. Right - View toward the southwest along the protected portion of the Todds Point peninsula. Rock revetment installed in 1977.**

LIDAR (Light Detection and Ranging) elevation data collected in March 2003 were obtained from the National Oceanic and Atmospheric Administration (NOAA) Coastal Services Center web site <http://maps.csc.noaa.gov/digitalcoast/data/coastallidar/index.html> and contoured to produce Figure 4. The contours clearly indicate the low relief nature of the peninsula, with most elevations along the unprotected stretch of the shoreline at approximately +0.9 meter NAVD88 (North Atlantic Vertical Datum of 1988) (Figure 4). Most of the rest of the area is below +1.7 meters elevation NAVD88. The three sided rectangle with lower elevations located in the lower right portion of the figure is an excavated farm pond. Extending to the northwest toward the protected shoreline is a shallow drainage ditch that is has an elevation in the +1.2 meter range. The rectangular farm pond and drainage ditch are also apparent in the black and white aerial photo (Figure 2).

In Figure 4 the section of shoreline that is protected with the revetment is indicated by the heavy black line. The unprotected northeastern shoreline has a jagged appearance due to the gridding and contouring procedure used to create the map, and does not represent the actual shoreline location. The LIDAR data were not used to indicate the shoreline position or specific configuration, only the elevation of the land surface used in the calculation of eroded sediment volumes on the peninsula.

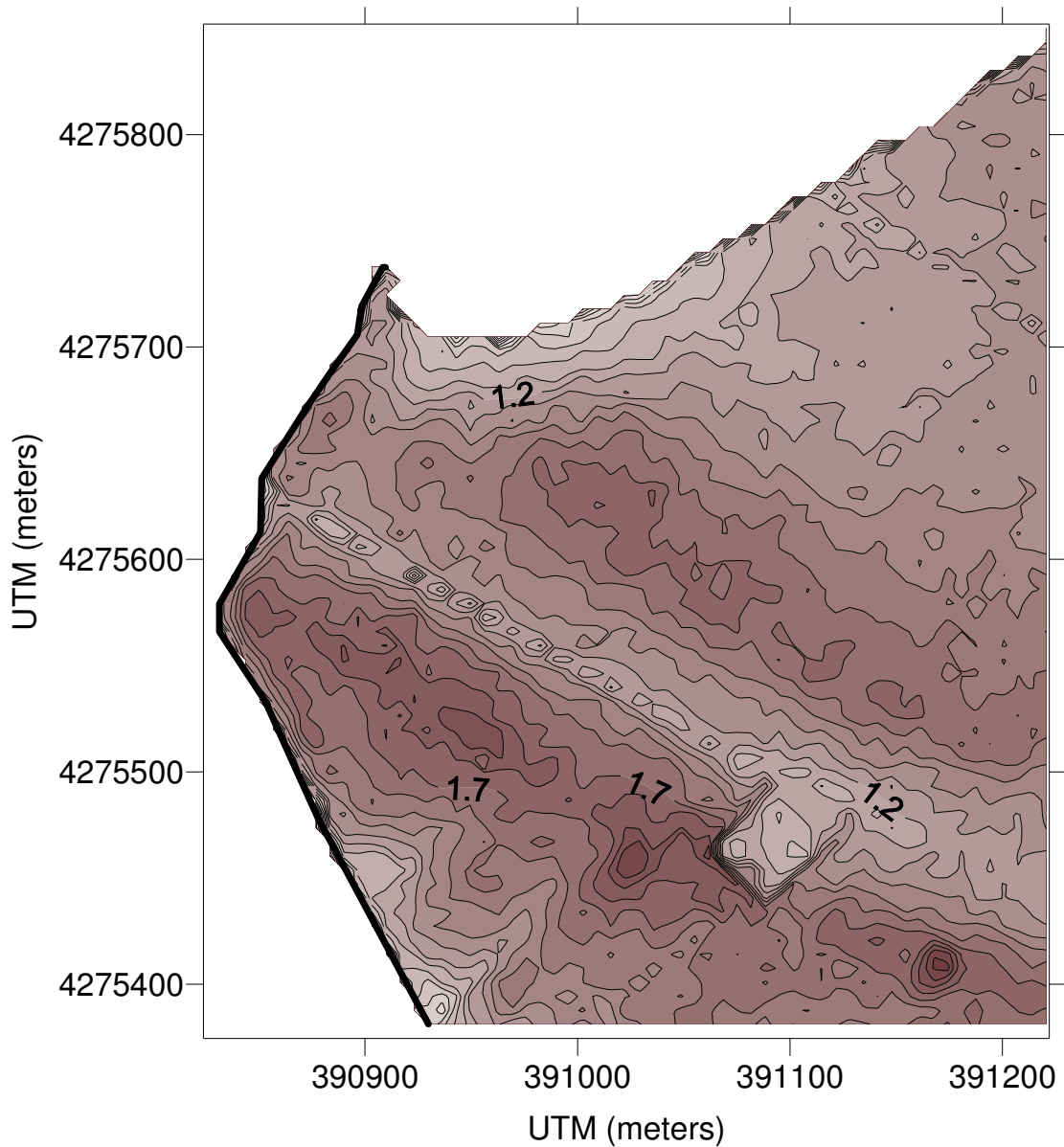


**Figure 4. Contoured 2003 LIDAR data of the Todds Point intensive study area. Contour interval 0.1 m NAVD1988. The western shore section protected by stone revetment is indicated by the heavy black line. The unprotected shore section, facing north, is not delineated by a shoreline, and the scalloped nature of this shore is an artifact of the contouring procedure.**

## METHODS

### Geomorphic and Geological Studies

Shoreline location data at the study site were collected using an Ashtech Reliance Precision GPS (Model SCA-12S; L1 code and carrier). Data were post-processed using internal software and posted satellite offsets obtained from the Global Positioning System Information website. Horizontal location accuracy of the post-processed data is in the sub-centimeter range.

Bathymetric data were collected using an Ashtech Reliance Precision GPS (model SCA-12S; L1 code and carrier) and a Knudsen 320B/P dual frequency echosounder with sounding frequencies of 200 KHz and 28 KHz. The echosounder transducer is a KEL771 dual frequency transducer with a 200 KHz beam angle of 4 degrees and a 28 KHz beam angle of 29 degrees. The echosounder generated 0.2 millisecond acoustic pulses for bottom recognition at a rate of 2 Hz. The transmitted acoustic wave reflected off the density gradient separating the water column from the bottom sediment. The time of the returned acoustic wave received by the transducer is converted to depth using a speed of sound in water of 1500 m/sec. At an average vessel speed of 4 knots, a depth sounding was collected approximately every 1.0 m along the survey track-lines. This data was stored along with the GPS location and positional latency in a laptop computer. Navigation was provided through a Lowrance GlobalNav 212 GPS interfaced to a Lowrance DGPS beacon receiver. A Starlink MRB-2 DGPS receiver provided DGPS signals to the Ashtech Reliance GPS system. DGPS differential corrections broadcast by the United States Coast Guard provided a real-time horizontal accuracy of 1 to 2 m [3 to 6 feet].

Bathymetric data were corrected for changes in water level during the survey period, by referencing to a water level recorder placed at the study site. The water level recorder was surveyed to a local survey point whose vertical elevation was determined using the Ashtech GPS over a long temporal baseline. Data from the water level recorder were compared to the NOAA tide station at Cambridge (Station ID: 8571892) over the deployment period (Figure 5). The comparison between the Cambridge observed and the Todds Point observed data are shown to be quite close, indicating that the Todds Point water level and bathymetric data had good vertical accuracy and confidence. Relatively minor excursions of the Cambridge observed tide beyond that at Todds Point occurred during particularly elevated or depressed water levels apparent on Figure 5. The differences likely were associated with local wind forcing events. Constriction of the Choptank River between the Todds Point and the Cambridge tide station locations may have produced these relatively minor differences in water elevation.

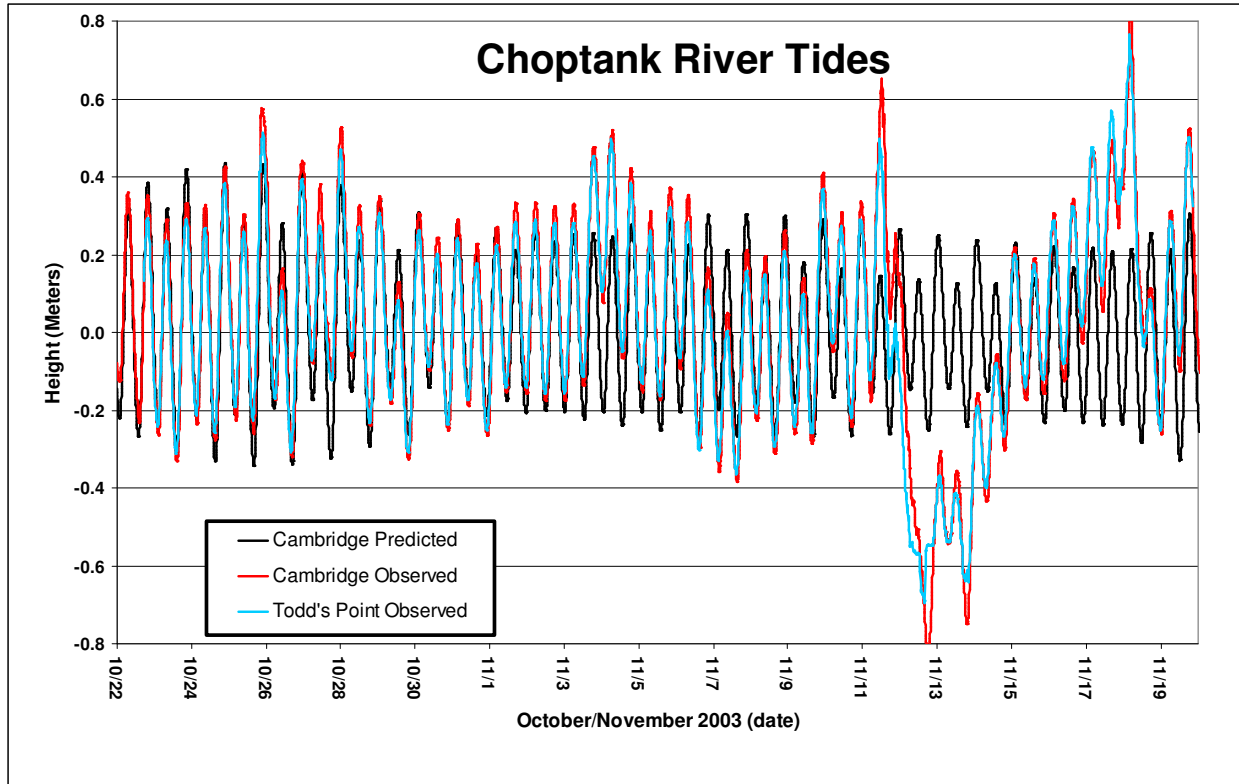


**Figure 5. Comparative plot of the NOAA Cambridge Tide Station (ID: 8571892) predicted and observed water levels with the Todd Point Tide Station observed water level for the period 10/22/2003 – 11/20/2003.**

Sediment samples from eroding banks were collected in 2003. At each sampling site, UTM coordinates were recorded using a Ashtech Reliance Precision GPS (model SCA-12S; L1 code and carrier) interfaced to a Starlink MRB-2 DGPS receiver which obtained Differential GPS signals. At each bank sampling location the sampling site and adjacent shore was described, as well as the actual sediment samples collected at each location. All sampling sites were photographed (Appendix).

At exposed eroding banks, multiple samples were collected from the eroding face if visually distinct sediment strata were apparent; otherwise a single sample was collected. Sediment samples were collected by inserting a 10 to 15 cm length of clear, cellulose acetate butyrate (CAB) plastic core liner (6.7 cm diameter) horizontally into the eroding bank face. The core liner was extracted and the ends trimmed such that the inside of the tube was completely filled with sediment. All sample tubes were capped and labeled and refrigerated until processing. The Appendix includes the field collection and description sheets for each bank sediment sample location.

Bottom sediment samples were collected offshore of the Todds Point area adjacent to both the protected and the unprotected shores using a Dietz-Lafond grab sampler that retrieves a layer of surficial sediment approximately 10 cm thick. Sample location was determined using the same equipment as outlined above for the bathymetric data collection.

Bank samples collected using the cellulose-acetate-butyrate (CAB) core tube were extruded in the laboratory and weighed. The sample was then homogenized. Exactly ¼ of the sample, by weight, was placed in a drying vessel, dried at 65°C, and then reweighed. The remaining ¾ of the sample was saved for grain size analysis and archival purposes.

Water content was calculated as the percentage of water weight to the total weight of wet sediment, as follows:

$$\% H_2O = \left( \frac{W_w}{W_t} \right) \times 100 \quad (1)$$

where  $W_w$  = the weight of water, in grams, and  $W_t$  = the weight of wet sediment, in grams.

Dry bulk density ( $\text{g/cm}^3$ ) was calculated as the dried weight (g) of the subsample divided by ¼ of the volume of the entire bank sample with the volume calculated from the length and diameter of the core tube for each sample.

Grain size analyses for both the bank samples and the bottom grab samples followed the same laboratory procedure. As part of this process the samples underwent a cleaning process to remove soluble salts, carbonates, and organic matter, which may interfere with the dispersal of individual sediment particles and, thereby, the subsequent separation of the sand and mud fractions. All sediment samples were treated first with a 10% solution of hydrochloric acid (HCl) to remove carbonate material, such as shells, and then with a 6% to 15% solution of hydrogen peroxide ( $\text{H}_2\text{O}_2$ ) to remove organic material. A 0.26% solution of the dispersant sodium hexametaphosphate ( $(\text{NaPO}_3)_6$ ) was then added to ensure that individual grains did not flocculate during subsequent analysis.

For each sample, the sand fraction was separated from the mud fraction by wet-sieving through a 4-phi mesh sieve (0.0625 mm, U.S. Standard Sieve #230). The sand fraction (particles > 0.0625 mm diameter) was dried and weighed. The mud fraction (sediment passing through the #230 sieve) was analyzed using a pipette technique to determine the proportions of silt and clay (Krumbein and Pettijohn, 1938). The mud fraction was suspended in a 1000- ml cylinder in a solution of 0.26% sodium hexametaphosphate. The suspension was agitated and, at specified times thereafter, 20 ml pipette withdrawals were made. The rationale behind this process is that larger particles settle faster than smaller ones. By calculating the settling velocities of different sized particles, withdrawal times can be determined. At the time of withdrawal, all particles larger than a specified size have settled past the point of withdrawal. Sampling times were calculated to permit the determination of the total amount of silt and clay (finer than 4 phi; 0.0625 mm diameter) and clay-sized (finer than 8 phi; 0.004 mm diameter) particles in the suspension. Withdrawn samples were dried at 60°C and weighed. From these data the percentages of sand, silt, and clay, by dry weight, were calculated for each sample. A subset of samples were analyzed as replicates for quality assurance purposes.

## Historical Shoreline Mapping and Erosion Rate Estimation

For this project, historical shorelines of the entire tidal Choptank River (including the study site at Todds Point) were mapped and used to estimate historical rates of shore erosion. Recent changes in shoreline locations were determined using two data sources:

- 1) The most recent Coastal Survey maps (topographic or T-sheets) produced by the National Ocean Service (NOS), a branch of the National Oceanic and Atmospheric Administration (NOAA); and
- 2) a digital wetlands delineation based on photo interpretation of 1988-1995 digital orthophoto quarter quadrangles (DOQQs).

The NOS (formerly the U.S. Coast and Geodetic Survey) is charged with surveying the coastline of the United States. NOS *Coastal Survey* maps, also known as topographic or T-sheets, are special use, planimetric maps that define the shoreline and alongshore natural and manmade features, including rocks, bulkheads, jetties, piers, and ramps. *Coastal Survey* maps are generally acknowledged to be the most accurate source of historical shoreline data (Anders and Byrnes, 1991; Shalowitz, 1964). They are often used in litigation to determine property ownership, to enforce regulatory mandates, and to estimate rates of shoreline change. The datum of “mean high water (MHW)” is used as the plane of reference for the shoreline.

The most recent shoreline vectors were digitized from the *Coastal Survey* maps, at scales of 1:5,000, 1:10,000, or 1:20,000 by the Maryland Geological Survey. Depending on the specific area in the Choptank the NOS shorelines utilized were mapped in the years between 1934 and 1975. The shorelines were merged and clipped to 7.5-minute USGS topographic quadrangle boundaries, which are reported in Table 1. The original T-sheets boundaries do not necessarily coincide with the quadrangle extents. Therefore, some quadrangles have multiple historical shorelines listed.

The more recent shorelines, dating from 1988 to 1995 were extracted from existing wetlands vectors, previously delineated for DNR over 1:1,000-scale digital orthophoto quarter quadrangles (DOQQs). MGS contracted the services of EarthData International (EDI) of Gaithersburg, Md., to interpret shorelines from DOQQs covering the region. An example of the historical shorelines for the Todds Point area are shown in Figure 6.



**Figure 6. Historical shorelines in the Todds Point area projected on a 1994 color Infrared Digital Orthophoto Quarter Quadrangle (DOQQ) image. The green line indicates the location of the shore in 1847, and the tan line in 1942.**

In Table 1, shorelines in each 7.5 minute quadrangle are listed with an ID and an associated date. In calculating rates of change, the most recent field edit date reported by the NOS was used. Digital orthophoto quarter quadrangles (DOQQs) were the ultimate source of the most recent (1992-1995) shorelines. “DOQQ Date” is the date on which the photography was flown. Historical shorelines for comparison and calculation of erosion rates were available as far upriver as the “Choptank Wetlands Preserve” just below the Route 331 (Dover Road) bridge.

**Table 1. Sources of Historical Shorelines, Choptank River, Maryland (grouped by USGS 7.5' Quadrangle).**

Quadrangle	Historical T-sheet		DOQQ	
	ID	Date(s)	ID	Date
Cambridge	T-5808	1940	NE, NW, SE, SW	1995
	T-8243	1943		
Claiborne	T-5708	1937	NE, NW	1992
	T-5723			
	T-8257	1942	SE, SW	1994
	T-11717	1961		
	TP-00842	1975	NW, SW	1994
	TP-00843			
	TP-00845			
	TP-00846			
	TP-00848			
	TP-00849			
	T-8244	1944		
Easton	T-8259	1942	NW, SE, SW	1995
Hudson	T-8241	1942	NE, NW, SE, SW	1994
Oxford	T-8249	1942	NE, NW, SE, SW	1994
Preston	T-8251	1944	NE, NW, SE, SW	1995
St. Michaels	T-5708	1937	NE, NW	1992
	T-8258	1942	SE, SW	1994
Tilghman	T-5723	1937	NE, NW, SE, SW	1994
	T-8248	1942		
	T-12083	1961		
	T-12084	1962		
	T-12086			
	T-12087	1962		
Trappe	T-8250	1942	NE, NW, SE, SW	1995

Many fastland areas of the Chesapeake Bay including the Choptank estuary have been protected from continued erosion by the construction of shore protection structures in the form of bulkheads or revetments. At the present time, these fastland areas are no longer contributing inorganic sediment to the estuary because of these protective structures, even though the historical shoreline mapping effort may show a change of shoreline location over the period of reference. This is simply due to the fact that the protective structure or structures may have been constructed at some point between the mapping of the two shorelines, thereby altering the historical erosion rates. For instance, if, over a 50-year period, a shoreline has retreated 50 m, the rate of erosion equals  $-1$  m/yr. However, if, after 25 years, a bulkhead had been erected along the reach, halting shoreline retreat, the 50 m of erosion would have occurred over a period

of 25 years, not 50. The actual rate of erosion would be  $-2$  m/yr before bulkhead construction and 0 m/yr afterwards. There is no existing database of information that indicates when a shore protective structure was constructed. As a consequence, determining the current delivery of sediment from fastland erosion required eliminating those lengths of shoreline where protective structures are located. In 2003-2004, the Virginia Institute of Marine Science (VIMS) surveyed waterfront shoreline of the Choptank River under contract to the Maryland Department of Natural Resources. This survey identified those sections of shoreline protected by structures along with other shore specific information. Data was provided by VIMS to MGS for use in this study, and is available on-line at [http://ccrm.vims.edu/gis\\_data\\_maps/data/index.html](http://ccrm.vims.edu/gis_data_maps/data/index.html). Shorelines that were protected by shore parallel structures, contiguous with the fastland (e.g. bulkheads or revetments) were excluded from the historical erosion rate calculation, because those sections of shoreline are no longer contributing sediment from fastland erosion. The survey conducted by VIMS indicated that of 328 kilometers of shoreline surveyed in the Choptank, 140 kilometers were protected. Nearly 43% of the Choptank River tidal shore had been hardened as of 2003-2004.

Shoreline rates of change were then calculated from the digital shorelines using the Digital Shoreline Analysis System (DSAS), a computer program written and supported by two researchers at the U.S. Geological Survey (Danforth and Thieler, 1992). DSAS created a "baseline" 50 m inland of the most landward shoreline, inserted nodes at 20-meter intervals along the baseline, and constructed a straight-line transect from each node, perpendicular to the baseline and across the available shorelines. For each consecutively dated pair of shorelines intersected by a transect, DSAS computed a rate of change by dividing the distance between the two shorelines by the time elapsed between them. In the Choptank River where two sets of recent historical shorelines were mapped as listed in Table 1, DSAS calculated annual rates of change for 10,270 transects. The annual volume of sediment delivered from fastland erosion in each unprotected reach was then calculated by multiplying the reach length, by the annualized erosion rate and the bank height. Bank height was estimated from examination of USGS topographic maps in combination with the information contained in the VIMS shoreline inventory database.

### **Nearshore Resuspension Measurements**

From 10/23/2002 – 11/21/2002, and again from 10/24/2003 – 11/21/2003, a bottom mounted tripod was deployed off of Todds Point in approximately 2 m (6.6 ft) MLW depth (see Table 2 for locations). These time periods were chosen because of the high likelihood of strong northwest winds with associated shore erosion and resuspension. The tripod, known as the Shallow Water Acoustic Turbulence Tripod (SWATT; Figure 7), was developed for similar deployments in the Pocomoke River, where it was used successfully several times. It uses a Sontek Hydra Acoustic Doppler Velocimeter (ADV) to measure bursts of 3-dimensional velocity and pressure sampled at 10 hz for 7 minutes each half hour, and has sufficient memory and battery life to last approximately one month. It was paired with a slower sampling temperature/conductivity sensor with an external optical backscatterance sensor to provide time series of tidal/wind forced current, surface waves, turbulence, temperature, salinity, and turbidity. It was deployed at Todds Point at an offshore reference location to characterize offshore currents, incoming waves, tidal height, and offshore turbidity.

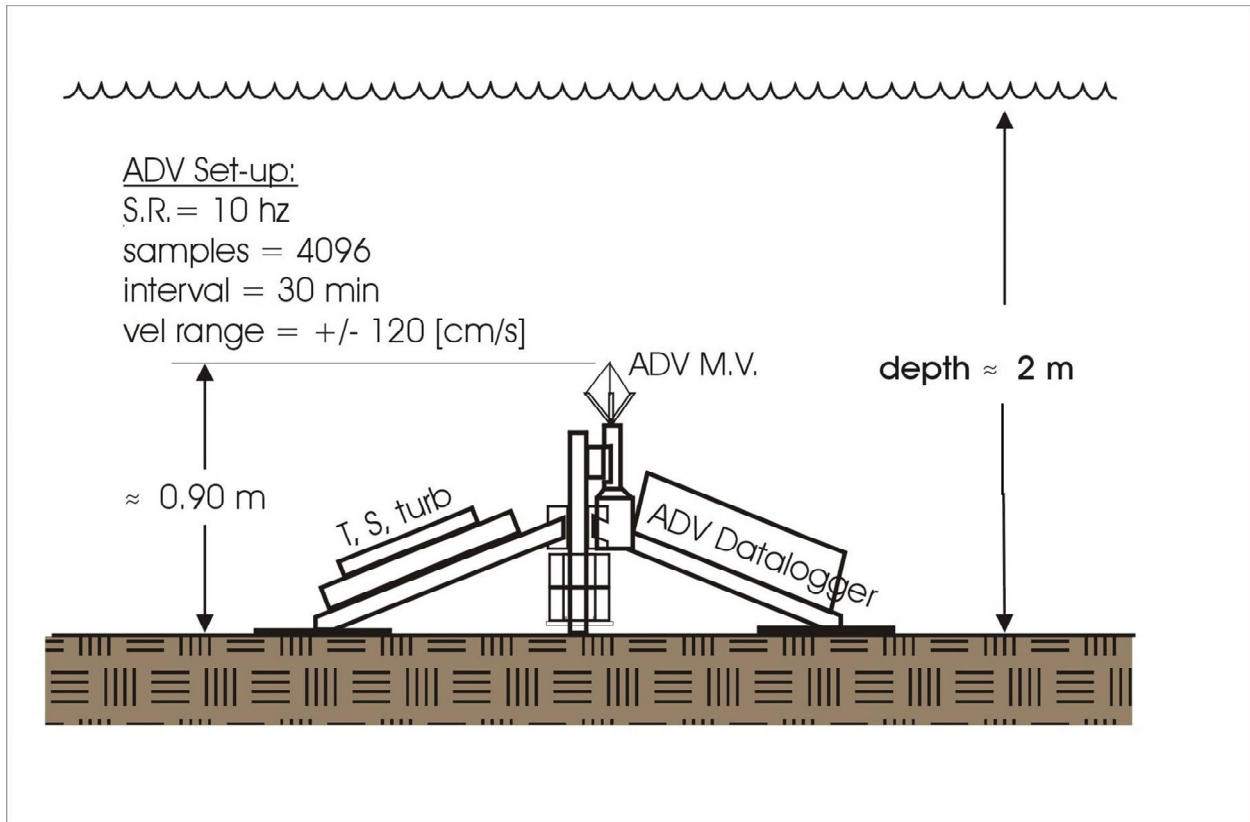


**Figure 7. Schematic of SWATT bottom tripod, deployed offshore.**

Closer to shore Conductivity/Temperature/Turbidity recorders were attached to vertical poles at 2 locations in 2002 and 3 locations in 2003 (Table 2). These instruments were deployed just far enough offshore to remain submerged at Mean Lower Low Water (MLLW), one off of the eroding shore, one off the armored shore, and the third in 2003 further down the armored shore. They were sampled at 5 minute intervals.

The time series of physical energy were compared to the time series of turbidity to determine the source of increases in turbidity, using the phasing between forcing and response as an indicator of local processes versus advection. Salinity and temperature are useful tracers in this regard as well. This technique was used successfully by Sanford (1994) on a similar data set to determine the influence of surface wave resuspension at a shallow site in upper Chesapeake Bay.

Hydrographic surveys in the mooring vicinity were carried out at approximately weekly intervals during the deployment, using the HPL SeaBird Sealogger CTD with auxiliary turbidity sensors (Figure 8). The CTD was deployed from a 25 ft. motorboat for offshore sites and strapped to the bottom of a kayak for nearshore locations. During the kayak surveys, a recording GPS sensor was used to provide location data for positioning of the hydrographic data. Collection of water samples during these surveys allowed calibration of the turbidity sensors. The hydrographic surveys provided a spatial context for the moored observations. Survey dates were occasionally adjusted to capture storm events. All survey dates are listed in Table 2.

**Table 2. Locations and times for resuspension studies.**

Field Sampling Event	Date/Time UTC	Northing	Easting	Notes
<b>2002 Resuspension Study</b>	Oct 23, 2002 to Nov 21, 2002	4277660 4275540	389700 391100	Bounding Coordinates
Offshore site ADV and CTT	Oct. 23, 2002 16:25 to Nov. 21, 2002 21:00	4276254	390618	Deployment
Unprotected site CTT	Oct. 23, 2002 17:45 to Nov. 21, 2002 17:31	4275750	390971	Deployment
Protected site 1 CTT	Oct. 23, 2002 18:12 to Nov. 21, 2002 19:07	4275677	390832	Deployment
Sles101 CTD survey	Oct. 23, 2002 19:25 to Oct. 23, 2002 21:45	4277660 4275540	389700 391100	Mapping survey
Sles102 CTD survey	Oct. 31, 2002 17:40 to Oct. 31, 2002 20:39	4277660 4275540	389700 391100	Mapping survey
Sles103 CTD survey	Nov. 7, 2002 17:12 to Nov. 7, 2002 19:46	4277660 4275540	389700 391100	Mapping survey
Sles104 CTD survey	Nov. 14, 2002 17:00 to Nov. 14, 2002 20:11	4277660 4275540	389700 391100	Mapping survey
Sles105 CTD survey	Nov. 21, 2002 16:10 to Nov. 21, 2002 20:28	4277660 4275540	389700 391100	Mapping survey
<b>2003 Resuspension Study</b>	Oct 24, 2003 to Nov 21, 2003	4277660 4275540	389700 391100	Bounding Coordinates
Offshore site ADV and CTT	Oct. 24, 2003 15:55 to Nov. 21, 2003 16:15	4276286	390636	Deployment
Unprotected site CTT	Oct. 24, 2003 17:45 to Nov. 21, 2003 17:00	4275748	390983	Deployment
Protected site 1 CTT	Oct. 24, 2003 16:50 to Nov. 21, 2003 16:50	4275706	390849	Deployment
Protected site 2 CTT	Oct. 24, 2003 17:06 to Nov. 21, 2003 16:45	4275570	390789	Deployment
Sles201 CTD survey	Oct. 24, 2003 18:38 to Oct. 24, 2003 21:25	4277660 4275540	389700 391100	Mapping survey
Sles202 CTD survey	Nov. 7, 2003 17:44 to Nov. 7, 2003 20:20	4277660 4275540	389700 391100	Mapping survey
Sles203 CTD survey	Nov. 12, 2003 19:00 to Nov. 12, 2003 21:27	4277660 4275540	389700 391100	Mapping survey
Sles204 CTD survey	Nov. 14, 2003 20:44 to Nov. 14, 2003 21:42	4277660 4275540	389700 391100	Mapping survey (aborted)
Sles205 CTD survey	Nov. 20, 2003 16:26 to Nov. 20, 2003 18:36	4277660 4275540	389700 391100	Mapping survey

**Key:**

- ADV** - Acoustic Doppler Velocimeter
- CTT** - Conductivity, Temperature, and Turbidity recorder
- CTD** - Conductivity, Temperature, Depth + Turbidity



**Figure 8. Left - CTD with OBS-3 turbidity sensor attached to bottom of kayak; Right – P. Dickhudt carrying out a kayak survey nearshore.**

### **Settling Velocity Experiments**

A series of laboratory experiments were carried out in late April 2004 to characterize changes in the size and settling velocity of particles from the Todds Point site that might be introduced into the water column from shore erosion or resuspension. These experiments utilized 1 cubic meter, 1 m deep mesocosms at HPL, originally developed for an EPA sponsored research program (Figure 9). Mixing paddles in these tanks were designed and tested to produce controllable, realistic levels of water column turbulence. The present study took advantage of an artifact of the mixing design; it produces an unrealistically low bottom shear stress at realistic water column turbulence levels, which prevents resuspension of deposited sediments (Crawford and Sanford 2001). However, at higher mixing levels, the entire tank is homogenized and there is no net deposition of fine sediments, although sands and coarser sediments are deposited.



**Figure 9. 1 cubic meter mesocosm used for settling experiments.**

Samples of bottom sediments and eroding shoreline soils were slurried in 2 um filtered Choptank River water using an electric paint stirrer. The slurries were introduced into the mesocosms at a high mixing rate, after which the mixers were turned down to produce a turbulence level of approximately  $1 \text{ cm}^2/\text{sec}^2$ , typical of near-bottom tidal conditions in Chesapeake Bay. One complete experiment was carried out for each sediment/soil sample. Downing and Associates OBS-3 backscatterance sensors were deployed in the tanks at 0.25 and 0.75 meters above the bottom. A Sequoia Instruments LISST-100C laser particle sizing instrument was deployed at 0.5 meters above the bottom. Time series of OBS turbidity, LISST transmissivity, and LISST particle size distribution were recorded at 1 sec intervals for 3-5 hours, until most of the sediment had settled. Suspended sediment samples were collected periodically for calibration of the optical sensors. Water temperature and conductivity were also measured for each experiment using a Seabird Sealogger CTD.

The data were analyzed to estimate changes in the size distribution and bulk settling velocity of the particle assemblage over the duration of each experiment. The bulk settling velocity  $w_s(t)$  was estimated from

$$\frac{dc}{dt} = -\frac{w_s}{h}c \quad (2)$$

Where  $c$  is the average concentration of suspended sediment in the tank and  $h$  is the tank depth. The LISST data were analyzed according to standard protocols (Sanford et al 2005).

### **Exploratory Modeling**

The estimates of long term erosion rate from shoreline positions in successive charts provide a good long term framework for the short term studies. Estimates of annual erosion from local shoreline surveys in October 2002 and November 2003 provide a shorter term framework that integrates over the 13 months of the study. However, the shoreline surveying techniques available for this project were not sufficiently accurate to measure the influence of each event during the intensive studies. It is doubtful that any existing technique is sufficiently accurate for this purpose. In addition, the measurement programs carried out for this project do not allow detailed extrapolation to previous (or future) conditions. To address these issues, the applicability of shore erosion models developed in the coastal engineering literature was explored, modified slightly to better reflect the conditions of this study site.

Dean (1991) provides a comprehensive summary of equilibrium beach profile approaches in coastal engineering. These concepts were developed mostly for sandy beaches, whose profile shapes continually adjust to changing wave climate and sea surface elevation but tend to return to a central equilibrium. This central equilibrium can exist because the majority of the sand volume is conserved, though it can be moved significantly onshore or offshore. In this sense, erosion of the dominantly fine grained shore sediments at Todds Point is different because most of the fine material appears to be ultimately lost offshore. However, the equilibrium beach profile approach provides a starting point for the modeling efforts.

Dean (1991) quotes a long known (e.g., Bruun 1954) central tendency for the equilibrium beach profile to be described by an equation of the form

$$h_{eq} = Ay^{2/3} \quad (3)$$

where  $h_{eq}$  is the equilibrium depth as a function of offshore distance  $y$ , and  $A$  is an empirical constant.  $A$  tends to be related to the sediment grain size, with values  $< 0.05$  for sediments finer than sands (Dean 1991). Both  $h_{eq}$  and  $y$  have units of m in Equation 3. Equation 3 assumes that  $h_{eq} = 0$  at  $y = 0$ , but at Todds Point the mean tide level is 0.5 m up the eroding bank face, so Equation 3 was modified to

$$h_{eq} = 0.5 + Ay^{2/3} \quad (4)$$

Dean further quotes a formula for the change in the equilibrium shoreline location due to a combination of waves and storm surge,

$$\Delta y_{eq} = -W \left[ \frac{0.068H_b + S}{B + 1.28H_b} \right] \quad (5)$$

where  $W$  is the surfzone width,  $S$  is surface elevation relative to mean tidal level,  $B$  is the height of the bank (or berm) at the shoreface, and  $H_b$  is the breaking wave height. Miller and Dean (2004) express these quantities as functions of time and change the values of the constants in the equation to convert from mean breaking wave height  $H_b$  to significant wave height  $H_s$ . Inserting a correction term for the 0.5 m offset of mean tide above the base of the bank, the final equation takes the form

$$\Delta y_{eq}(t) = -W(t) \left[ \frac{0.106H_s(t) + 0.5 + S(t)}{B + 2.0H_s(t)} \right] \quad (6)$$

$W$  is a function of wave height and total water depth, so it can be expressed as

$$W = \max \left[ \left( \frac{\frac{H_s}{0.78} - 0.5 - S}{A} \right)^{3/2}, 4 \times H_s \right] \quad (7)$$

where equation 4 and a standard relationship between breaking wave height and water depth have been combined with a minimum breaking zone of 4 wave heights set to account for direct wave breaking against the shore face when the water is too deep to have a normal surf zone.

Miller and Dean (2004) further allow for time variation in the shoreline by writing an equation for the rate of change of shoreline position  $y(t)$  as a function of the difference between the equilibrium position corresponding to current conditions and the actual present position,

$$\frac{dy(t)}{dt} = k [\Delta y_{eq}(t) - y(t)] \quad (8)$$

where  $k$  is a constant of proportionality with units of  $\text{time}^{-1}$ . Their numerical solution of Equation 8 allows for an arbitrary specified forcing function  $\Delta y_{eq}(t)$ .

A problem with Equation 8 is that it assumes a fixed frame of reference for shoreline position, i.e., a fixed long term equilibrium position to which the shoreline tends to return. This makes sense for a sandy beach where sand volume is conserved, but not for a shore composed of finer grained silts and clays that remain in suspension and are removed by currents. Under these conditions, the shore never builds out again and continuing erosion is the only possible outcome. This problem was dealt with by redefining the frame of reference at each point in time; i.e., by setting  $y(t) = 0$  at all times for strictly eroding shores. Thus, Equation 8 was modified to

$$\frac{dy(t)}{dt} = k \Delta y_{eq}(t) \quad (9)$$

Equation 9 was solved numerically using a semi-implicit recursive equation very similar to that presented by Miller and Dean (2004):

$$y_{n+1} = y_n + \alpha (\Delta y_{eq,n} + \Delta y_{eq,n+1}) \quad (10)$$

where  $\alpha = k \Delta t / 2$ .

An alternative to the equilibrium beach profile ideas can be formulated based on the work of (Wilcock et al., 1998), who considered factors influencing coastal bluff erosion along Calvert Cliffs, MD. They consider the rate of bluff recession due to direct wave breaking against the shoreface, as opposed to the surf zone processes described above. They show that the rate of recession seems to be related to the ratio of the maximum expected wave pressure  $P_{me}$  to the shoreface strength  $\tau_s$ , both with units of Pa, with more frequent exposure to high values of this ratio corresponding to the fastest eroding shores. The maximum expected wave pressure is highest over a limited range of the ratio of the wave height to the water depth at the shoreface,

$$0.85 < x < 1.35, \text{ where } x = \frac{H_s}{S + 0.5} \quad (11)$$

This expression for  $x$  is written specifically for Todds Point by substituting in  $S + 0.5$  for total water depth at the shoreline. In this range, the maximum expected wave pressure is approximately

$$P_{me} = 35 \rho g H_s \quad (12)$$

where  $\rho$  is the density of water and  $g$  is acceleration due to gravity. The wave induced pressure is much less below this range of  $x$  (non-breaking waves) and above this range of  $x$  (waves break

before striking the shoreface), with the pressure due to already broken waves somewhat larger than that due to unbroken waves. This behavior may be approximated over the entire range  $0 < x < \infty$  by

$$\frac{P_{me}}{35\rho gH_s} = f(x) = [2.5x \exp(-0.91x)]^3 \quad (13)$$

which is shown in Figure 10. The functional shape shown has an average value of 1 over the interval  $0.85 < x < 1.35$ , drops off quickly below this range, and drops off slightly less quickly above this range. It is non-unique (there are many other functions with similar behavior) but it offers a reasonable form for testing.

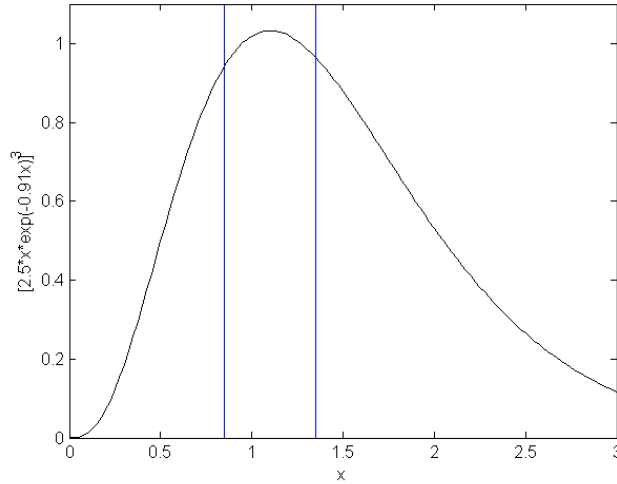


**Figure 10. Plot of the structure function  $f(x)$  in Equation 13.**

Using Equation 13 and lumping all of the other unknowns and constants (such as the strength of the Todds Point bank and the rate of recession per unit forcing) into one tunable parameter  $K$ ,

$$\frac{dy(t)}{dt} = -KP_{me}(t) \quad (14)$$

Equation 14 is solved using the same method as the solution for Equation 9,

$$y_{n+1} = y_n - \beta(P_{me,n} + P_{me,n+1}) \quad (15)$$

Where  $\beta = K\Delta t/2$ .

Equations 10 and 15 were calculated for the 13 month period encompassing the Todds Point observations by assembling estimates of wind speed and direction, corresponding wave height, and tidal height, then calculating Equations 7 and 6 for each point in time to yield an estimate of  $\Delta y_{eq}(t)$  as the forcing function in Equation 10 and a similar estimate of  $P_{me}$  as the forcing function in Equation 15. Wind speed and direction were obtained from a CBOS surface buoy that was deployed at Castle Haven in the lower Choptank during approximately 8 of the 13 months, augmented by data from the continuous Thomas Point Light weather station ([www.ndbc.noaa.gov](http://www.ndbc.noaa.gov)). Winds from both sensors were corrected to 10 m reference height following the methods of Lin et al. (2002a, 2002b). The Thomas Point winds were then adjusted to match the Choptank buoy winds when the records overlapped, and the GLERL Chesapeake Bay wave model of Lin et al. (2002a, 2002b) was run for the lower Choptank and adjacent Chesapeake Bay. The model estimated significant wave heights from the grid point nearest to Todds Point were stored for comparison to wave data from the SWATT tripod when available, and for input into Equations 6 and 7. Tidal height data were obtained from the NOAA Cambridge, MD tide gauge (<http://tidesandcurrents.noaa.gov>), and were adjusted as necessary to match the tidal height data from the SWATT tripod when available. The adjusted tidal height data were used to represent  $S(t)$  in Equations 6, 7, and 11.

## RESULTS

### Geomorphic and Geologic Studies

The upland adjacent to the lower Choptank River in Dorchester, Talbot and Caroline Counties is primarily a low lying level to gently rolling plain with elevations less than 20 feet, composed of unconsolidated sediments of Miocene, Pleistocene and recent ages. The surficial geology of both Dorchester and Talbot Counties has been mapped, and the sediments comprising the shores consist in large part the Pleistocene age Kent Island Formation (Owens and Denny, 1986a, b). Sediments of this formation were deposited in a previous generation of the Chesapeake Bay. Due to deposition in an environment similar to the present Chesapeake Bay, the sediments of the Kent Island formation are largely fine grained silts and clays with some intermixed sands. The slightly coarser sands may be present in thin lenses and pockets throughout the formation. The Kent Island Formation has been described as "Interbedded silt, clay, and sand, with abundant organic matter in places. Clayey and silty sediments underlie most of Dorchester County..."(Owens and Denny, 1986a). On the north shore of the Choptank River the Kent Island Formation underlies most of the western part of Talbot county (Owens and Denny, 1986b). They also note that the base of the unit is commonly placed at a thin gravel bed that overlies a black clay of the Miocene age Chesapeake Group (undifferentiated).

The Chesapeake Group (undifferentiated) was mapped along some segments of both the north and south shores of the Choptank River locally upriver of Chlora Point on the north shore and Horn Point on the south shore (Owens and Denny, 1986a, b). Sediments comprising the Chesapeake Group are described as "Largely interbedded....massive to finely laminated silt and clayey silt and....fine-grained....loose, micaceous slightly feldspathic quartz sand." The Chesapeake Group is interpreted as Miocene age open-ocean shelf deposits. Although the Miocene sediments were mapped as undifferentiated by Owens and Denny, previous works specifically identified these sediments as comprising the Choptank Formation along the banks of the Choptank River (Cleaves et al., 1968). The Choptank Formation is most readily identified in exposures along Calvert Cliffs on the western side of the Chesapeake.

Locally at Castle Haven Point, Hambrooks Bar, and in the vicinity of Cambridge the shore consists of the Pleistocene age Parsonsburg Sand, which as its name implies, consists of loose sand, but is locally peaty near its base (Owens and Denny, 1986a). The formation is however quite thin with a maximum thickness extending only 4 meters into the subsurface. The Parsonsburg Sand does not extent into Talbot County. The Parsonsburg is thought to represent small dune formations and winnowed sands of aeolian origin (Owens and Denny, 1986a)

Portions of the shore are composed of Holocene tidal marshes, particularly upstream of Cambridge on the Dorchester County side of the river, and upstream of the town of Choptank on both the Talbot County and Caroline County portions of the river. Tidal marsh sediments consist largely of organic matter with a large portion of silt and clay sized particles, along with thin lenses of sands (Owens and Denny, 1986a, b).

Given the surficial sediment mapping that has been completed, it is apparent that shore erosion along the majority of the shore of the Choptank River is likely to supply largely fine

grained sediments to the tidal portions of the estuarine river. Only in those limited areas where the Parsonsburg sand are present, primarily in the vicinity of Cambridge, is shore erosion likely to contribute much sand size material to the estuary.

Bank samples along the shore in the embayed section of the Choptank River were collected at eight locations including three at the Todds Point intensive study area (Figure 11). Sample collection at additional locations, particularly facing areas with long fetch in the lower Choptank River, was attempted, but the extent of shoreline protective structures precluded obtaining additional samples. For example no unprotected shorelines existed in the Broad Creek area or south east of the Deep Neck Point samples to Benoni Point at the mouth of the Tred Avon River. Analysis of data presented in the Maryland Shoreline Situation Reports developed by the Virginia Institute of Marine Sciences indicates that fully 43% of the Choptank River shore was protected by bulkheads and revetment at the time of the shoreline surveys in 2003-2004 (Berman et al.; 2003, 2005).

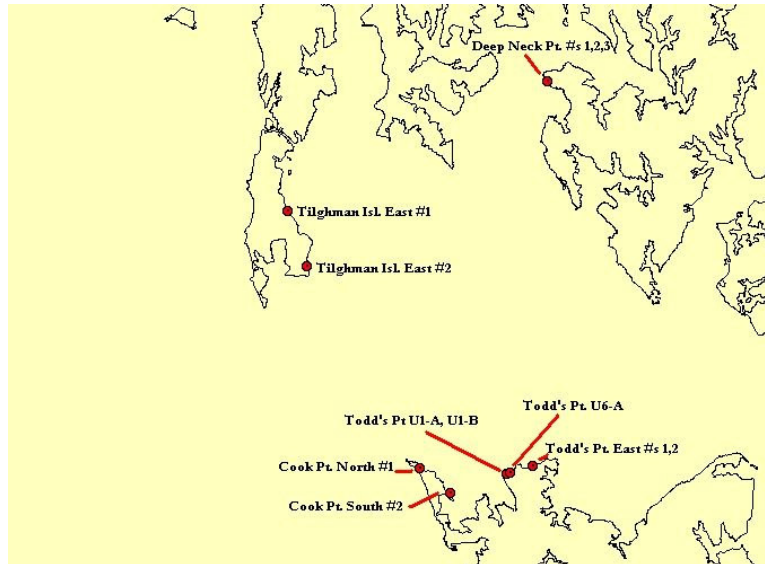


**Figure 11. Location of bank samples collected in the Choptank River estuary. Detailed site descriptions and field sheets for each location appear in the Appendix.**

At each location samples were collected from identifiable strata in the eroding bank. If the bank consisted of a single apparent stratum then only one sample was collected from that location. In locations where more than one stratum was present, samples were collected from each strata. Field sheets for all sampling locations are reproduced in the appendix. Each field sheet contains a description of the site, coordinate information, photographs, and detailed information on the specific sample collection sites. A total of eleven samples were analyzed for grain size information, dry bulk density and total carbon, sulfur and nitrogen (Table 3). Although not utilized in this interpretation, the percent by dry weight of total nitrogen, carbon, and sulfur is included in the Table for completeness.

Excluding the sample at Tilghman Island East #2, which was collected in the bank of a tidal marsh, all the samples were from the eroding faces of low height vertical banks. The samples were collected from below the soil horizon and represented the fresh face of the eroding shoreline sediment. Excluding the marsh sample the average dry bulk density of the eroding banks was 1.61 g/cc and the sand content was 19%. Finer grained silts and clays constituted 81% of the sample on average, with 53% silt and 28% clay (Table 3). The single marsh sample had a dry bulk density of 0.32, with a sand content only slightly greater than 2% and the remainder composed of fine grained silts, clays and organic materials.

**Table 3. Bulk properties and sediment composition of shore samples collected along the shore of the Choptank River. Sample locations shown in Figure 11.**

Bluff Sample ID	Dry Bulk Density (g/cc)	% Sand	% Silt	% Clay	Shephard's Classification	Total Nitrogen % wt	Total Carbon % wt	Total Sulfur % wt
Cook Point North #1	1.49	9.17	64.66	26.17	Clayey-Silt	0.017	0.117	0.000
Cook Point South #2	1.63	7.91	70.94	21.15	Clayey-Silt	0.016	0.102	0.000
Deep Neck Point #1	1.90	7.66	55.96	36.39	Clayey-Silt	0.039	0.455	0.054
Deep Neck Point #3	1.92	31.84	42.40	25.76	Sand-Silt-Clay	0.022	0.161	0.000
Todds Point U1-A	1.54	33.65	36.49	29.87	Sand-Silt-Clay	0.019	0.110	0.015
Todds Point U1-B	1.62	55.41	25.73	18.86	Silty-Sand	0.016	0.077	0.000
Todds Point U6-A	1.60	3.81	65.38	30.81	Clayey-Silt	0.030	0.298	0.028
Todds Point East #1	1.50	2.34	69.85	27.81	Clayey-Silt	0.024	0.281	0.000
Todds Point East #2	1.40	23.55	51.90	24.54	Sand-Silt-Clay	0.023	0.191	0.000
Tilghman East #2	1.46	15.96	44.14	39.90	Clayey-Silt	0.042	0.188	0.013
<b>Average</b>	<b>1.61</b>	<b>19.13</b>	<b>52.74</b>	<b>28.13</b>		<b>0.025</b>	<b>0.198</b>	<b>0.011</b>
<b>Marsh Sample ID</b>								
Tilghman East #1	0.32	2.34	69.85	27.81	Clayey-Silt	0.818	14.252	1.636

Eroding banks in the Choptank have a much higher fine grained (silt and clay) component and a higher dry bulk density than the average for all eroding banks in the Maryland portion of the Chesapeake reported in Hill et al. (2003), which is consistent with the fine-grained characterizations of the geologic formations in the counties surrounding the Choptank River. The average for eroding banks in the entire Maryland portion of the Chesapeake Bay was 44% sand, and 56% silt plus clay, with a bulk density of 1.38 g/cc versus 19% sand and 81% silt plus clay with an average bulk density of 1.61 g/cc in the Choptank (Table 3). The bulk property and grain size distribution of eroding banks in the Choptank River will be utilized to calculate the sediment delivered from shore erosion later in this report.

The bulk density and grain size distribution of the single marsh sample from Tilghman Island is significantly lower than values reported for eroding marsh banks in Maryland in Hill et al. (2003). They reported an average bulk density of 0.62 g/cc, with 22% sand, 44% silt plus clay, and 34% organic matter. The values reported by Hill et al. (2003) are consistent with other samples collected from eroding marsh bank faces in the Maryland portion of the Chesapeake

(Kearney and Stevenson, 1991; Kearney et al., 1994; Kearney and Ward, 1986), but are more consistent with the characteristics of interior marsh samples from Maryland (Kearney et al., 1994; Stevenson et al., 1985). Although this sample was collected locally, its characteristics are inconsistent with other data sets, and probably not representative of eroding marsh faces in the Choptank. Thus, in calculating the sediment contribution of eroding marshes to the Choptank estuary the values reported in Hill et al. (2003) and substantiated by the previous reports cited above, will be utilized. These values are: 0.62 g/cc bulk density, 22% sand, 31% silt, 13% clay and 34% organic matter.

Two general bank locations were sampled along the eroding north shore of Todds Point. Two specific locations at the intensive study area and another slightly to the east (Figure 11). Full site descriptions are provided in the Appendix. All samples were collected from the vertical face of eroding banks that were between 0.5 and 1.0 meter in height, and fronted by small sandy beaches at the base. A typical bank face and a portion of the abutting beach is shown in Figure 12.



**Figure 12. Eroding bank face on the north shore of Todds Point East Station.**

In cross section, the beach sand present at all locations on the north side of Todds Point forms a small triangular wedge that overlies the harder more erosion resistant Pleistocene Kent Island Formation. The sand wedge thins away from the shore, and the Pleistocene sediments are exposed at low tide at variable distances from the shoreline depending on the amount of sand present (Figure 13). The exposed Kent Island sediments are shown in close up in Figure 14. Further from shore low amplitude shore parallel sand bars are often present with the Kent Island Formation exposed in the bar troughs (Figure 15).



**Figure 13. Eroding bank at Todds Point fronted by a wedge of beach sand and exposed Kent Island Formation in the middle of the figure**



**Figure 14. Eroding Pleistocene age Kent Island Formation, exposed at low tide, bottom of figure. Toward the top, a thin deposit of sand fills an eroded depression in the sediment surface.**



**Figure 15. Nearshore low amplitude sand bars exposed during an exceptionally low tide at Todds Point on November 14, 2003. Kent island Formation sediments are exposed in the bar troughs. The vertical pole in the upper left quadrant holds a CTT sensor.**

The eroding bank at the Todds Point study area has sediment characteristics that are similar to the overall characteristics of the Choptank River estuary (Table 4). The dry bulk density is within a tenth of a g/cc, and the percentages of the various particle sizes are all within 5% of the Choptank River average. The sand sized component is about 4% higher than the average for the Choptank, while the silt and clay sized fractions are about 3% and 2% lower respectively. The eroding bank characteristics of the Todds Point intensive study area can thus be considered fairly representative of the conditions at eroding banks throughout the estuarine portion of the Choptank River. Local erosion of sediments from this bank will be determined in a latter section of this report.

**Table 4. Bank sediment characteristics at the Todds Point Intensive Study area (extracted from Table 3).**

Bluff Sample ID	Dry Bulk Density (g/cc)	% Sand	% Silt	% Clay	Shephard's Classification	Total Nitrogen % wt	Total Carbon % wt	Total Sulfur % wt
Todds Point U1-A	1.54	33.65	36.49	29.87	Sand-Silt-Clay	0.019	0.110	0.015
Todds Point U1-B	1.62	55.41	25.73	18.86	Silty-Sand	0.016	0.077	0.000
Todds Point U6-A	1.60	3.81	65.38	30.81	Clayey-Silt	0.030	0.298	0.028
Todds Point East #1	1.50	2.34	69.85	27.81	Clayey-Silt			
Todds Point East #2	1.40	23.55	51.90	24.54	Sand-Silt-Clay			
<b>Average</b>	<b>1.53</b>	<b>23.75</b>	<b>49.87</b>	<b>26.38</b>		<b>0.02</b>	<b>0.16</b>	<b>0.01</b>

Figure 16 depicts the bathymetry at the Todds Point intensive study area utilizing data collected in the fall of 2002 as part of this study. Bathymetric data were again collected during the fall of 2003 in an attempt to assess depth changes over the course of the study year. However, depth differences were below the limits of data resolution and as a result no changes could be effectively mapped. Figure 16 also depicts the locations of three shore normal transects, each extending approximately 800 meters offshore. Two are located on the eastern part of the study area which had the unprotected shore and one on the western portion where the revetment provided protection from shore erosion. Also, shown is the location of the 1847 shoreline.

The nearshore zone slopes gently away from the shoreline, out to a distance of nearly 200 meters offshore where the 1.4 meter depth contour is located. The slightly irregular depth contours which include small closed contour lines in this region are attributed to the small amplitude sand bars which were shown in Figure 15 and were apparent in the air photo of the area (Figure 2). The slope then flattens noticeably between the 1.4 and 1.6 meter depth contour, which is located about 500 meters from shore. The slope increases slightly between the 1.6 and 2.0 meter depth contours, and then increases sharply beyond the 2.0 meter depth to the limits of the study area where depths exceed 3 meters. Waves approaching the study area from the northwest, approximately normal to the shoreline, encountered very similar depth profiles offshore of both the protected and the unprotected shore areas. The 2 meter and greater depths apparent on the southwestern side of the surveyed area represent the edge of a slightly deeper channel that connects Cook Point Cove with the Choptank River.

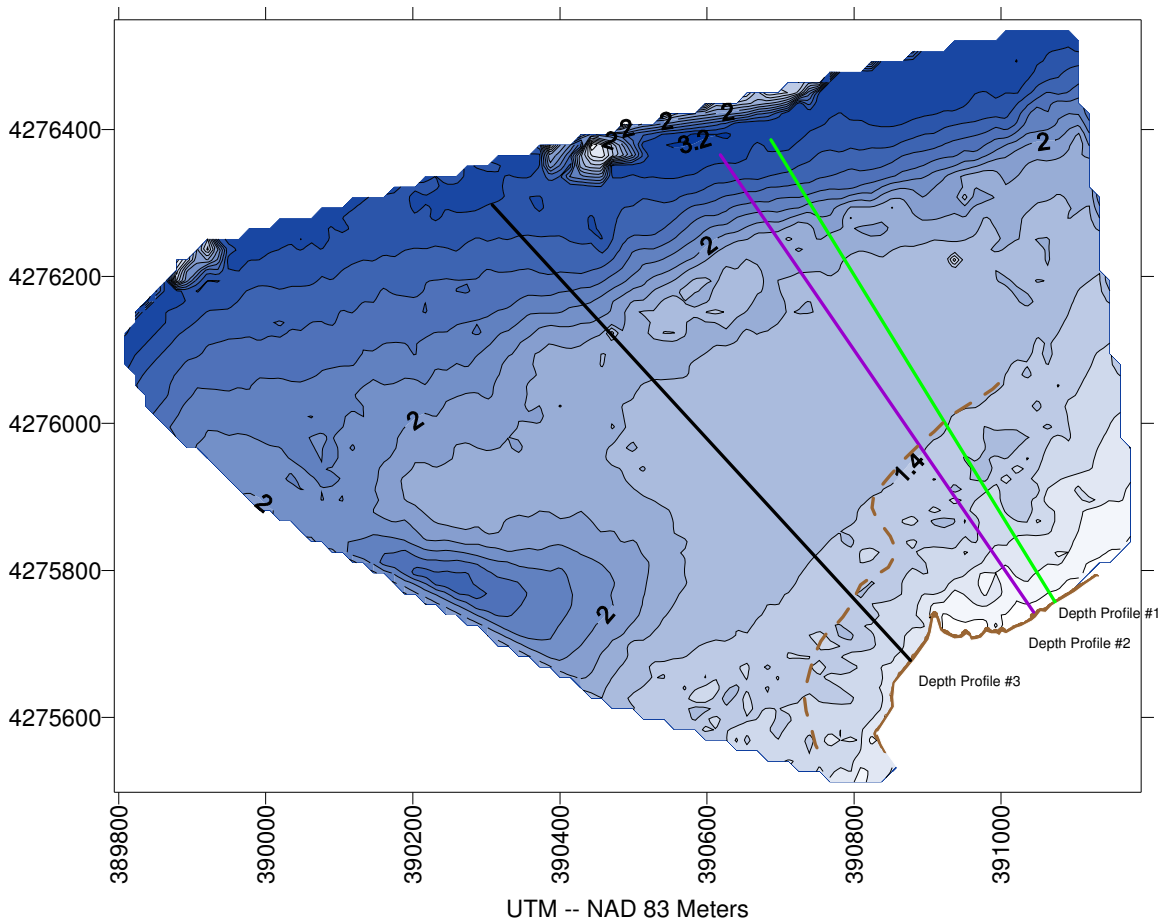


**Figure 16. Bathymetry offshore of the Todds Point intensive study area, collected in the fall of 2002. The 2002 shoreline is shown as the solid brown line, and the 1847 shoreline position is indicated by the dashed brown line located offshore. Locations of the three shore normal profiles shown in Figure 17 are also indicated. Contour interval 0.2 meters.**

Profile sections offshore of Todds Point are shown in Figure 17 for the three locations indicated in Figure 16. All of the profiles have a generally similar form as discussed above. There are two notable differences between profiles 1 and 2, on the unprotected shore, and profile 3, on the protected shore. Profile 3 is deeper adjacent to the shore, and Profiles 1 and 2 exhibit higher amplitude depth changes between 100 and 200 meters from shore than does Profile 3. Note that the vertical exaggeration of the figure emphasizes these differences.

Adjacent to the shore, Profile 3 exhibits depths about 0.3 meter greater than profiles 1 and 2, but continuing offshore the depths converge for all three profiles and beyond about 150 meters from shore are similar for all three. The greater depths immediately offshore on profile 3 are attributed to the continuation of erosion of the nearshore zone by wave action since the revetment was emplaced along this stretch of shore in 1977. The revetment successfully stopped erosion of the upland farmland on the peninsula, but subaqueous erosion continued since that time. The nearshore areas of Profiles 1 and 2, in contrast, are shallower, because this

unprotected shore has continued to erode and retreat over the same time period. At any particular point offshore the erosive action of waves and currents has had less time to remove sediments from the bottom and create greater depths. All profiles converge at about the 1.4 meter water depth. In water greater than about 1.4 meters the existing wave climate has less opportunity to erode bottom sediments, producing the broad shallow platform extending outward in all three profiles to between 500 and 600 meters offshore.

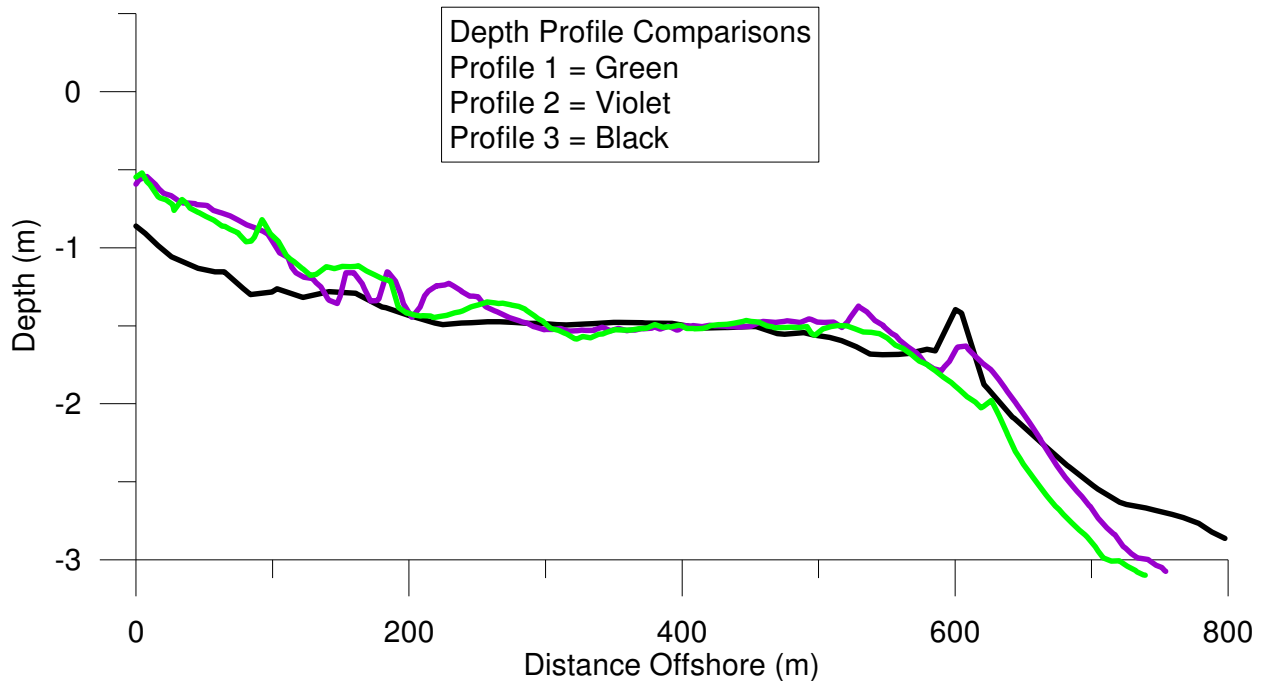


**Figure 17. Offshore depth profiles along the three shore normal transects shown in Figure 16. See text for details.**

The nearshore sand bars pictured in Figure 15 which was photographed on a day with exceptionally low tides produce the depth changes apparent on Profiles 1 and 2 out to about 200-250 meters offshore. Three bars are present on each profile, but the wavelengths are less across profile 2 than across profile 3. The bar amplitude of about 0.2 meter is similar across both profiles. It should be noted, however, that the gridding and contouring conducted on the raw depth data to produce the bathymetric contours results in some averaging and smoothing of the data sets, so not all the details of the profiles are retained. In any case, the low amplitude nature of these nearshore bars is apparent. In contrast, Profile 3 exhibits much less depth variability across the inner nearshore zone, and indeed the shore parallel bars may not even be present offshore of the revetment protected shore. The lack, or extreme low amplitude, of any nearshore bars along Profile 3 is attributed to a diminished sand supply to this area that resulted from the emplacement of the revetment to protect the shore from erosion. The source of sand from shore erosion has been removed, and large storm waves, though infrequent, effectively remove most of the sand on this platform. The sand is either transported in an offshore direction where it is deposited below the base of effective wave action or along the shore and out of the area.

Local erosion of the shore at Todds Point during the period of the intensive study was determined by locating the shoreline position with Differential GPS on two subsequent dates, October 24, 2002 and November 14, 2003. The unprotected stretch of the shore retreated landward an average of 2.48 meters over this period (Figure 18). The specific periods during which erosion took place in response to wind, wave and tide variations could not be determined, and the method represents an overall average. Given an average elevation of 0.9 meters (Figure 4) derived from LIDAR data, the total volume of land eroded above the water line was 630 cubic meters over the approximate one-year period.

In comparison, shore erosion of the unprotected shore between 1847 (shoreline position shown on Figure 16) and 2002 averaged 1.81 meters/year, about 2/3 of a meter less per year on average. The notably higher recent erosion rate could be due to any one or a combination of factors, including change in the erodability of the land, greater rate of sea level rise, change of land use from forest to farmland, greater exposure to storm waves as Cook Point eroded, or more storm events than average during the study period.

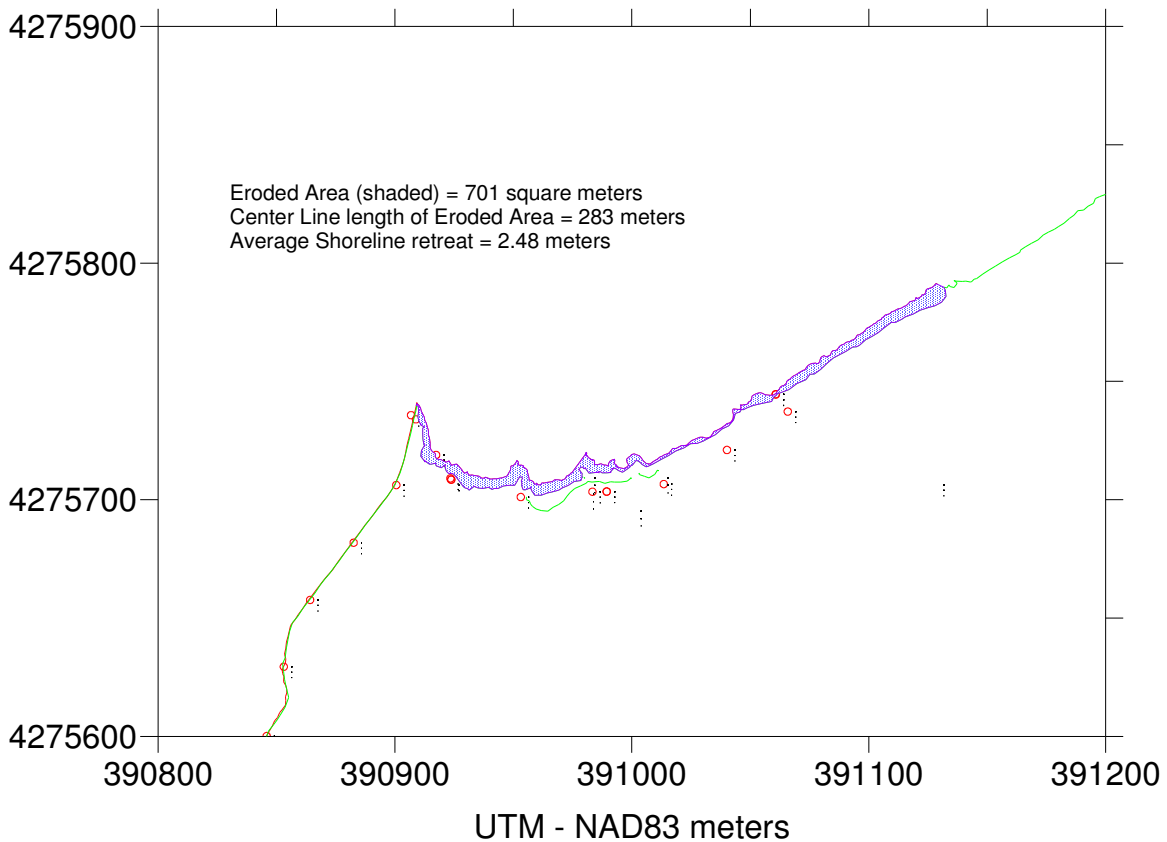


**Figure 18. Measured shore erosion over a one-year period at Todds Point shown by the blue stippled pattern. Red circles are control points. The shore in the lower left of the figure where no change is indicated is protected with stone revetment. The shore in the upper right was not measured on both dates, and no change is indicated.**

## Historical Shoreline Mapping and Erosion Rate Estimation

Data derived from the historic shoreline locations and erosion rates, the elevations and sediment properties of the eroding shore banks and the extent of hardened shorelines were combined to determine the overall contribution of sediment to the Choptank River estuary resulting from shore erosion. For each area, the two most recent shorelines were utilized to determine the historical erosion rate. Generally, the earlier shoreline utilized dated from the 1940's to the mid-1970's and the most recent from the mid-1990's (Table 1), thus spanning a period of approximately 30 to 50 years.. Erosion from shores protected by hardened structures (e.g. bulkheads, revetments) were eliminated from the calculation of upland erosion.

Traditionally, sediment delivery to tidal estuaries has been calculated from the linear retreat of the shore over time, often referred to as shoreline erosion, multiplied by the elevation of the land. However, this determination has neglected to take into account the erosion of the bottom in the shallow waters immediately offshore of the eroding sub-aerial land. From a property loss perspective, the basis of this determination is understandable, but from the perspective of the estuary and the total delivery of sediment to tidal waters, the adjacent shallow bottom erosion needs to be included. For the remainder of this report erosion of uplands is referred to as fastland erosion and erosion of the adjacent shallow water bottom is termed nearshore erosion. The sum of both the fastland and the associated nearshore erosion is collectively termed “shore erosion” (Figure 19).

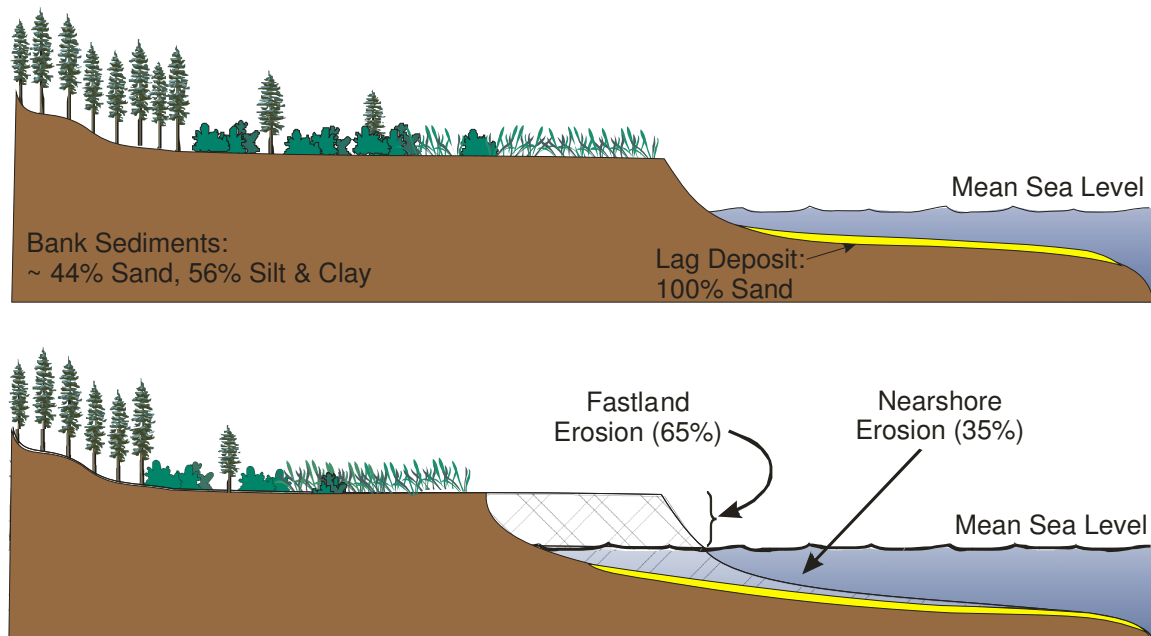


**Figure 19. Representation of the contribution of both the fastland and near-shore components in delivering sediment due to shore erosion. Not to scale.**

Fastland erosion rates over the recent past were calculated using the process outlined in the Methods section as discussed previously. However, a direct calculation of the associated nearshore erosion rate could not be determined because no comprehensive data set exists that indicates the amount of nearshore erosion that has historically taken place and bathymetric data to support an accurate determination is woefully inadequate. For example, only one digital data set of bathymetry exists for the Choptank River and that was collected in the mid-1940's. Clearly, nearshore erosion is taking place as indicated by the presence of navigable open water offshore of the current peninsula (Figures 6, 16). Therefore, it was necessary to derive an estimate of the nearshore erosion rates from the erosion rate of the adjacent fastland.

The U.S. Army Corps of Engineers shoreline erosion report (US Army Corps of Engineers, 1990), stated that fastland erosion accounts for 43% and nearshore erosion 57% of the sediment load delivered by tidal erosion in the Chesapeake Bay. However, no data was presented to support or verify this ratio. This ratio undoubtedly differs widely in various locations throughout the estuary and reflects a variety of determining factors such as sediment composition, shoreline elevation, offshore bathymetry, shoreline orientation, and land use among other factors. Based on the bathymetric work conducted at Todds Point, discussions with Scott Hardaway of the Virginia Institute of Marine Science and knowledge of nearshore bathymetry at other locations in the Maryland portion of the Bay, it has been estimated that a reasonable ratio of fastland to nearshore erosion averages 65:35 (Figure 19). This ratio was utilized in the analysis of shore erosion contributions to the tidal Chesapeake Bay for the entire estuary that was recently conducted for the Chesapeake Bay Program by the Maryland Geological Survey and staff of the Bay Program office.

The amount of nearshore erosion could be readily calculated for shorelines with unprotected fastland sections, simply by calculating the volume of fastland sediment eroded and applying the 65:35 ratio. However, in those areas where the fastland is protected by a hardened shoreline consisting of a bulkhead or revetment, nearshore erosion still occurs even though the fastland erosion has been halted as discussed previously and shown on Figure 17. To estimate the erosion from the nearshore region of a shoreline that had protected fastland, the following method was utilized. The fastland erosion rate for an adjacent reach of unprotected shoreline was calculated on a per unit shoreline length basis, and the associated nearshore erosion rate determined using the 65:35 ratio. This nearshore erosion rate was then applied to the length of the adjacent protected shoreline on a per unit shoreline length basis.

The prevailing understanding is that protecting a shoreline with a hardened structure may actually increase the erosion of the adjacent nearshore areas for two reasons. First, the hardened shoreline reflects incident wave energy back into the nearshore area where it increases the wave energy affecting the bottom. Second, protecting the shore eliminates a proximate source of sediment that could nourish and maintain beaches and blanket the adjacent bottom with a lag deposit of sand. The presence of the coarser sand sized sediment would provide a form of armoring, reducing the continued erosion of the underlying materials. However, the existence and degree of an increase in nearshore erosion due to the emplacement of a hardened shoreline structure has never been thoroughly documented (U.S. Army Corps of Engineers, 2002). Because of the lack of documentation, no increase in nearshore erosion was assumed to occur offshore of protected shoreline reaches.

Shorelines of the Choptank estuary were segregated into various sub-units to provide an estimate of the shore erosion in each portion of the system. The division was based, in part, on overall geomorphic characteristics of the sub-unit including, bank elevation and type, shore orientation, offshore bathymetry and fetch. The separate reaches are shown in Figure 20. This division process separated the Choptank River into upper, middle, and lower portions, plus the wide embayed section below Castle Haven Point. These are labeled Chopt 1 through 4 respectively. Each of the major tributaries on the north shore of the Choptank are also separated and labeled individually.

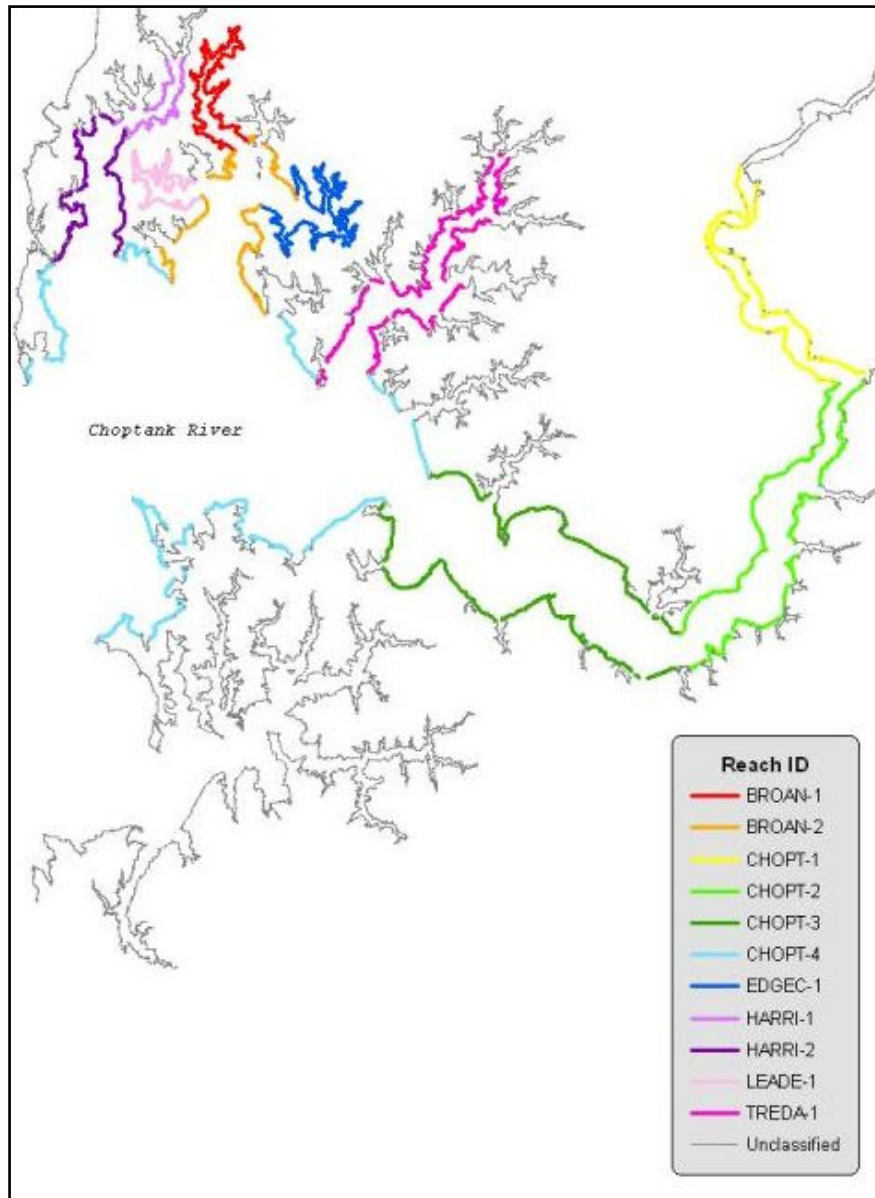


**Figure 20. Identification of the individual reaches in the Choptank River and tributaries for which shore erosion rates were calculated.**

The identified reaches differ widely in the amount of shoreline hardening that has been emplaced (Table 5), depending primarily on location within the estuary. The lowest percentages of shore protection occur in the upper reaches of the Choptank in reaches Chopt-1 (7%) and Chopt-2 (22%), where the river is narrow and there is no significant fetch. Given the lack of fetch one can assume that property owners do not feel compelled to spend significant monies on shore protection. However, immediately downriver in section Chopt-3 where the river widens notably shore protection increases to 52% of the total shoreline length, the third highest degree of protection reported in the table. The greatest amount of shore protection is emplaced in Broad Creek (Broan-2) with 69% of the shoreline hardened, and in the Tred Avon River with 64% protected. Both sections of Harris Creek (Harri-1 and Harri-2) have more than 50% of the shore hardened. Shoreline hardening in the lower reach of the Choptank (Chopt-4) is less than 50%. This section of the river has significant fetch and would appear to be a prime candidate for a greater amount of shore hardening. However, it was noted in the field work for this project that the north shore of the river, in Talbot County, had a very large degree of hardening, while along the more agricultural south shore in Dorchester County, there was little hardening. This apparently reflects the relative incomes of the residents in the two counties. Overall 39% of the tabulated Choptank River estuary shoreline was hardened. This percentage is slightly less than the 43% total reported in the VIMS report, which is explained by the different total shoreline extents considered (244 km in Table 5 v. 328 km in the VIMS report).

**Table 5. Total shoreline length and protected length for reaches shown on Figure 20.**

Reach ID	Total Reach Length (m)	Protected Length (m)	Protected Length (%)
BROAN-1	25,785	10,562	41
BROAN-2	22,273	15,305	69
CHOPT-1	32,224	2,190	7
CHOPT-2	37,329	8,351	22
CHOPT-3	38,439	20,150	52
CHOPT-4	51,435	22,592	44
EDGE-1	33,848	14,292	42
HARRI-1	11,837	6,427	54
HARRI-2	19,604	10,375	53
LEADE-1	19,707	7,617	39
TREADA-1	30,050	22,463	64
<b>TOTAL</b>	<b>244,424</b>	<b>91,983</b>	<b>39</b>

Within each reach the bank elevation was determined from the available topographic data presented on the associated USGS 15-minute quadrangle, and the extent of shore attached marshes was determined from the VIMS shoreline situation data sets, examination of air photographs, and information on the USGS quadrangles. Marshes were estimated to have an average elevation of 0.5 meters. The annual volume of fastland erosion, nearshore erosion, and total erosion for each reach shown in Figure 20 was calculated and reported in Table 6. Volumes were converted to mass of sediment separated into its various grain size components, utilizing the different bulk characteristics reported previously for banks and marshes discussed previously. Eroding banks were assumed to deliver no appreciable organic matter to the estuary, while eroding marshes consist of 34% organic matter. Results for each reach are reported in Table 6.

**Table 6. Volume and mass of sediment delivered from shore erosion to each of the Choptank River reaches identified in Figure 20.**

Reach ID	Fastland Volume (m <sup>3</sup> )	Nearshore Volume (m <sup>3</sup> )	Total Volume (m <sup>3</sup> )	Sand Mass (T/yr)	Silt Mass (T/yr)	Clay Mass (T/yr)	Organic Mass (T/yr)	Total Mass (T/yr)
BROAN-1	3,041	2,773	5,814	1,778	4,928	2,654	0	9,360
BROAN-2	2,355	4,898	7,253	2,149	5,877	3,156	87	11,269
CHOPT-1	11,976	7,434	19,410	5,146	13,386	7,110	984	26,627
CHOPT-2	9,283	10,026	19,309	4,752	11,892	6,260	1,437	24,341
CHOPT-3	6,966	11,034	18,000	5,279	14,377	7,713	283	27,652
CHOPT-4	32,512	39,273	71,785	19,979	53,179	28,390	2,462	104,010
EDGE-1	4,451	4,148	8,599	2,631	7,290	3,925	0	13,845
HARRI-1	1,206	1,421	2,627	804	2,227	1,199	0	4,230
HARRI-2	6,065	7,729	13,794	4,153	11,433	6,148	83	21,817
LEADE-1	1,853	1,627	3,480	1,064	2,950	1,588	0	5,603
TREDA-1	2,495	4,453	6,948	2,084	5,728	3,079	52	10,942
<b>TOTAL</b>	<b>76,807</b>	<b>87,145</b>	<b>163,952</b>	<b>43,807</b>	<b>116,734</b>	<b>62,334</b>	<b>5,249</b>	<b>228,125</b>

The lowest total sediment loads from shore erosion are delivered from the upper reaches of the small tributaries on the north shore of the Choptank, Harrison Creek (Harri-1) and Leadenham Creek (Leade-1). Combined these two tributaries deliver less than 10,000 metric tons per year into the estuary. Three other tributaries on the north shore each deliver about 10,000 metric tons per year, the upper and lower portions of Broad Creek (Broan-1 and Broan-2) along with the Tred Avon (Treda-1) and Edge Creek (Edge-1). The three upper reaches of the Choptank (Chopt-1, Chopt-2, Chopt-3) each deliver approximately 25,000 metric tons per year and the lower portion of Harris Creek (Harri-1) supplies just over 20,000 metric tons. By far the highest delivery is supplied by the lower open, embayed section of the Choptank River (Chopt-4) with over 100,000 metric tons eroded each year.

In total shore erosion processes, accounting for both fastland and nearshore erosion provide 228,125 metric tons per year of sediment, of which 179,068 metric tons is fine grained silts and clays that are more likely to be suspended in the water column, transported throughout the estuary and attenuating light penetration. For comparison, the USGS maintained River Input Monitoring station of the Choptank reports an average delivery of suspended sediment of 2,400 metric tons per year from a watershed of 290 km<sup>2</sup>, which averages to 8.28 metric tons/km<sup>2</sup>/year. This annual load per unit area can be scaled up to the entire watershed using the land surface for the Choptank tributary basin, reported by the Department of Natural Resources at 1,500 km<sup>2</sup>. This yields an estimate of 12,428 metric tons of fine grained suspended sediment entering the tidal waters of the Choptank from the watershed. Even though approximately 40% of the Choptank River shore is hardened, significantly reducing both the load of fine grained sediments to the estuary and eliminating miles of natural shore habitat, erosion of the fastland and associated nearshore areas in the Choptank still delivers a fine grained sediment load approximately 14 times the load estimated to be delivered from the watershed.

Locally, at the Todds Point intensive study area, the total delivery of sediment from the eroding fastland at the site was calculated over the duration of the study period from the shoreline retreat of 701 m<sup>2</sup> and a bank height of 0.9 meters (Figure 18). This yielded a sediment volume of 631 m<sup>3</sup> over the 386 days between the two shoreline measurements, or 1.63 m<sup>3</sup> per day. The total mass of sediment eroded from the fastland shore was calculated to be 965 metric

tons, or 2.50 metric tons/day. Using the local sand/silt/clay percentages at Todds Point of 24/50/26, the eroding fastland shore produced 0.60 metric tons per day of sand, 1.25 metric tons of silt, and 0.65 metric tons of clay sized sediments. Combined, 733 metric tons of fine grained sediments were supplied to the Choptank River waters by erosion of the unprotected Todds Point bank at the study area, at an average rate of 1.90 metric tons per day.

The presence of the mapped 1847 shoreline at the Todds Point study area (Figure 16) and the current bathymetric data from 2002 enables a calculation of the erosion that has taken place in the nearshore zone as the shoreline retreated over that time period. Figure 21 shows offshore Profiles 1 and 2 on the unprotected shore with that portion of the present day profile landward of the 1847 shoreline location highlighted in red. A slight smoothing function has been applied to this portion of the depth profile to minimize the effect of the nearshore bars on the resulting bathymetry and calculation. The shoreline at Profile 1 retreated a total of 280 meters since 1847 period. Assuming that the average land elevation on the eroded part of the peninsula was approximately 1.0 meter, similar to the present land elevation (Figure 4), the eroded fastland area above the water line is 280 m<sup>2</sup> in cross section (Figure 21 - top). Similarly for Profile 2 the shoreline retreated 263 meters and the eroded fastland area was 263 m<sup>2</sup> in cross section (Figure 21 - bottom). Below the water surface the nearshore zone continued to erode over the time period since 1847 and the eroded area seaward of the present day shoreline and below mean water level is 306 m<sup>2</sup> for Profile 1 and 276 m<sup>2</sup> for Profile 2. Averaging the eroded material values for both profiles indicates that at the Todds Point study area the nearshore erosion accounts for 52% of the total sediment load contributed to the estuarine waters by shore erosion while the fastland component accounts for the remaining 48%. Given the generally flat elevation of the upland portion of the peninsula (Figure 4) and the similar nearshore bathymetry seaward of the unprotected shoreline (Figure 16) these profiles are assumed to reasonably reflect the proportion of nearshore versus fastland erosion for the entire unprotected length of the peninsula.

Nearshore erosion at Todds Point accounts for 17% greater contribution of sediment than was assumed for the baywide average calculation. We speculate that the high amount of nearshore erosion in this area is due, at least in part, to the relatively low amount of sand present in the eroding sediments. The presence of significant sand on the bottom of the nearshore zone might serve to both reduce both the fastland erosion and the nearshore erosion by protecting the shore and contributing bottom sediments from the erosive action of waves.

The 48% fastland and 52% nearshore contribution to the total sediment load from shore erosion can be used to estimate the sediment erosion in the nearshore zone over the study period, even though the successive bathymetric surveys one year apart were unable to identify consistent depth changes in this region. Nearshore erosion yielded 1045 metric tons of sediment over the 386 days of the study period, with 251 metric tons being sand, 523 silt, and 272 clay sized materials. In total, the combined fastland and nearshore sediment load from erosion at Todds Point was 2010 metric tons over the study period; 483 metric tons as sand, 1006 metric tons as silt, and 523 metric tons as clay sized particles. The average sediment erosion per day was 5.21 metric tons, with 1.25 metric tons of sand, 2.61 metric tons of silt, and 1.35 metric tons as clays.

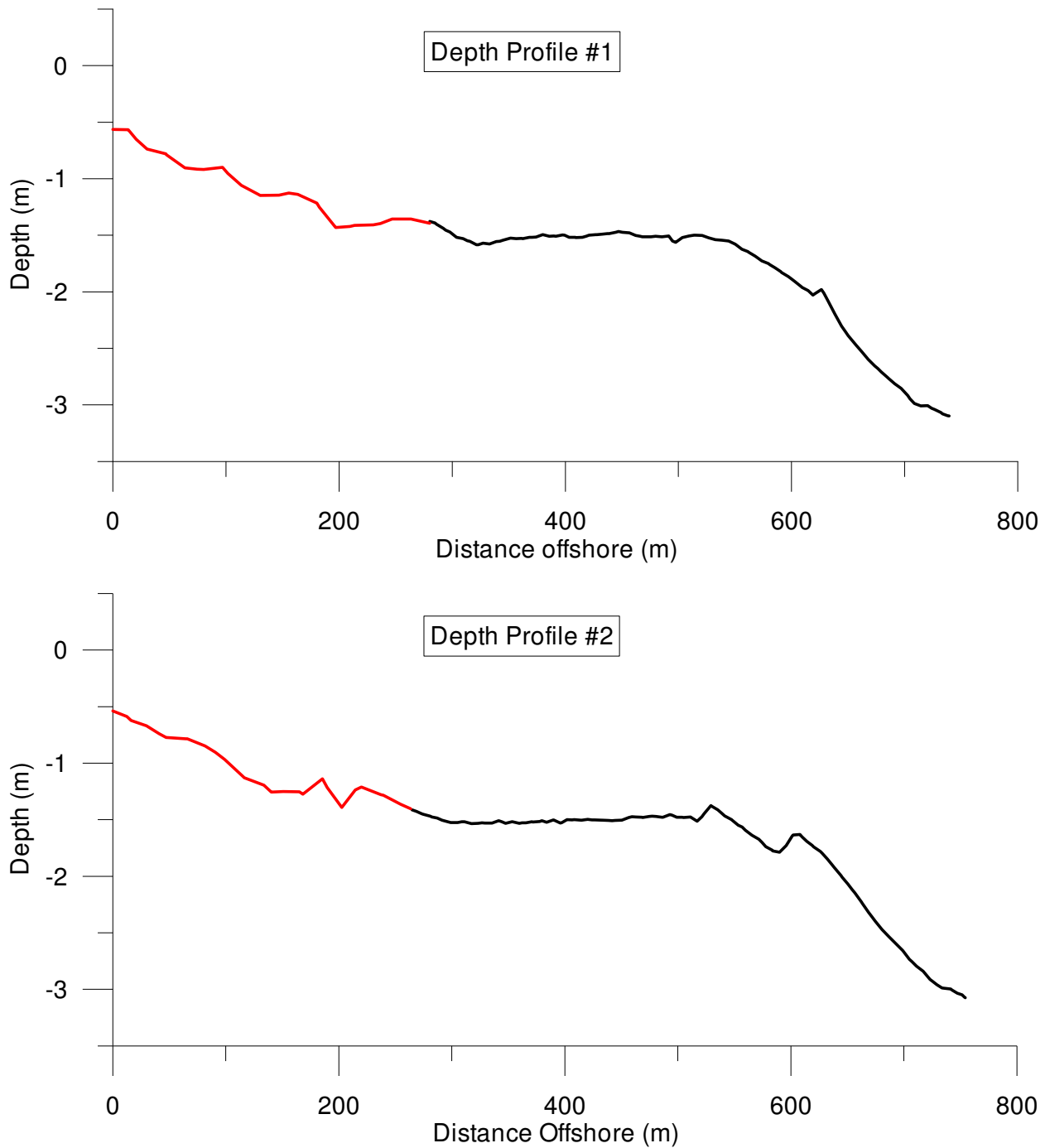


**Figure 21. Unprotected profiles 1 (top) and 2 (bottom) at the Todds Point study area with that portion shoreward of the 1847 shoreline highlighted in red.**

## Nearshore Resuspension Measurements

The locations of the moored sensor deployments are shown superimposed on a bathymetric map of the area offshore Todds Point in Figure 22. The conductivity, temperature, and turbidity sensors were all located approximately 0.25 meters above the bottom, while the wave and current data from the SWATT were collected approximately 0.9 meters above the bottom.

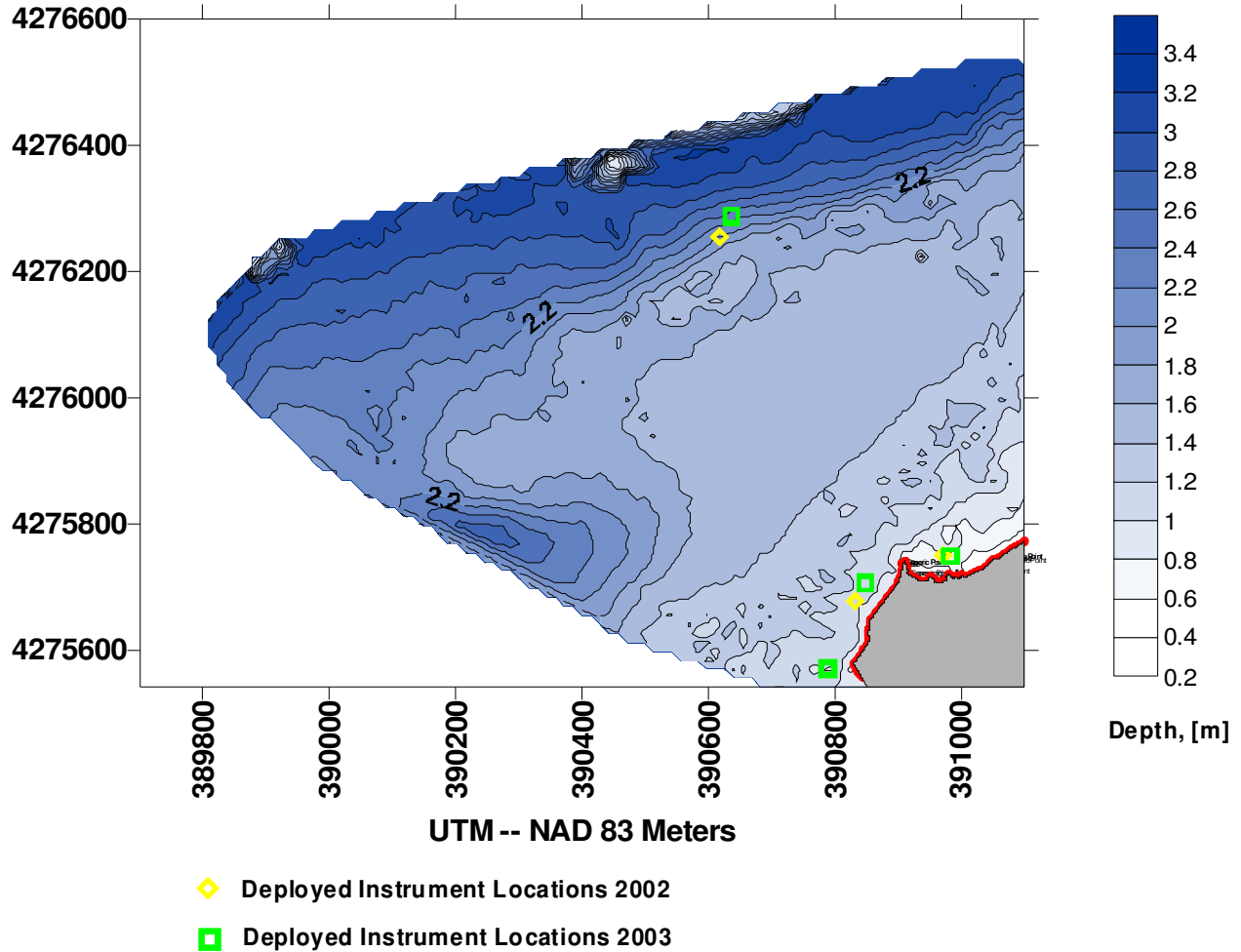
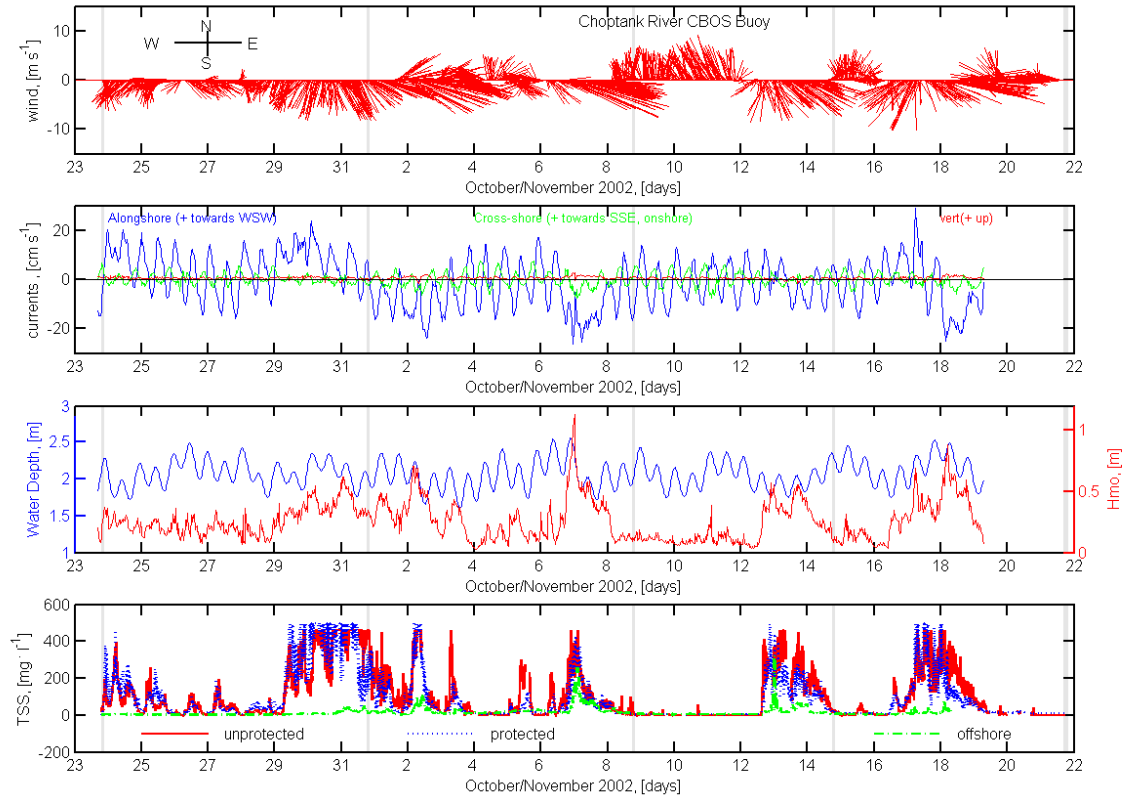


Figure 22. Bathymetric map of area offshore Todds Point with locations of moored sensor deployments shown for 2002 and 2003 field studies. The SWATT was deployed approximately 0.5 km offshore, with the CTT sensors deployed as close to shore as possible while still remaining submerged.



**Figure 23. Time series from moored sensors for the period of the 2002 Todds Point deployment. Upper panel - Choptank River CBOS buoy wind vectors, pointing in the direction towards which the wind is blowing. Second panel – Average currents from the SWATT ADV, resolved into alongshore and crossshore directions. Third panel – Significant wave height and water depth from the SWATT pressure sensor. Lower panel – Estimated TSS from calibrated turbidity measurements from all deployed sensors.**

Stack plots of Choptank River CBOS buoy wind, currents, waves, tidal height, and TSS from all available sensors are presented in Figure 23 for the entire period of the 2002 deployment. The data show that this period was, as hoped, punctuated by a series of strong N to NW wind events (wind blowing strongly onshore towards the S or SE), notably Oct 29-Nov 4, Nov 6-Nov 8, Nov 12-14, and Nov 16-19. Tidal currents were predominantly in the alongshore direction with speeds  $< 0.2 \text{ m s}^{-1}$ , augmented by wind-forced fluctuations. Few if any of the tidal current speeds measured at the tripod were sufficient to resuspend or erode significant amounts of sediment by themselves, and it is quite likely that the current speeds were even slower nearshore. Rather, waves approximately  $> 0.25 \text{ m}$  in height resulted in the largest nearshore TSS values ( $> 100 \text{ mg l}^{-1}$ ). Most of the time, in the absence of waves, nearshore TSS concentrations were  $< 10 \text{ mg l}^{-1}$ . Note that the absolute value of these low TSS estimates is somewhat questionable because of the lack of sensitivity and uncertainties in the calibrations of the OBS turbidity sensors in the low concentration range, but the predominance of very low turbidity/TSS without waves is clear. TSS levels at the unprotected and protected nearshore sites during wave events were usually difficult to distinguish, although levels at the unprotected site appeared to be

somewhat higher on occasion. TSS levels at the offshore SWATT site were usually lower, reflecting both the lack of an immediate shoreline erosion response and the deeper water depth, which isolated the bottom from wave activity relative to the nearshore site and reduced local resuspension.

Stack plots of wind, currents, waves, tidal height, and TSS from all available sensors are presented in Figure 24 for the entire period of the 2003 deployment. Once again, there were several strong wind events from the N to NW directions that resulted in very high nearshore TSS levels. The event periods for the 2003 deployment were Oct 28-30, Nov 7-10, Nov 13-16, and Nov 20. General conclusions from examining the overall 2003 time series are almost the same as those from 2002 above. Three interesting differences were that the extremely low tidal heights centered on Nov 14 resulted in relatively little nearshore turbidity because they exposed the bottom (as well as exposing the nearshore sensors) and isolated the shoreface (Figure 15), that the additional turbidity sensor further down the protected shoreface often seemed to show slightly lower TSS levels during events, and that the influence of fouling was apparent (uniquely) in the second protected side turbidity sensor record beginning on Nov 11 until it was cleaned on Nov 12.

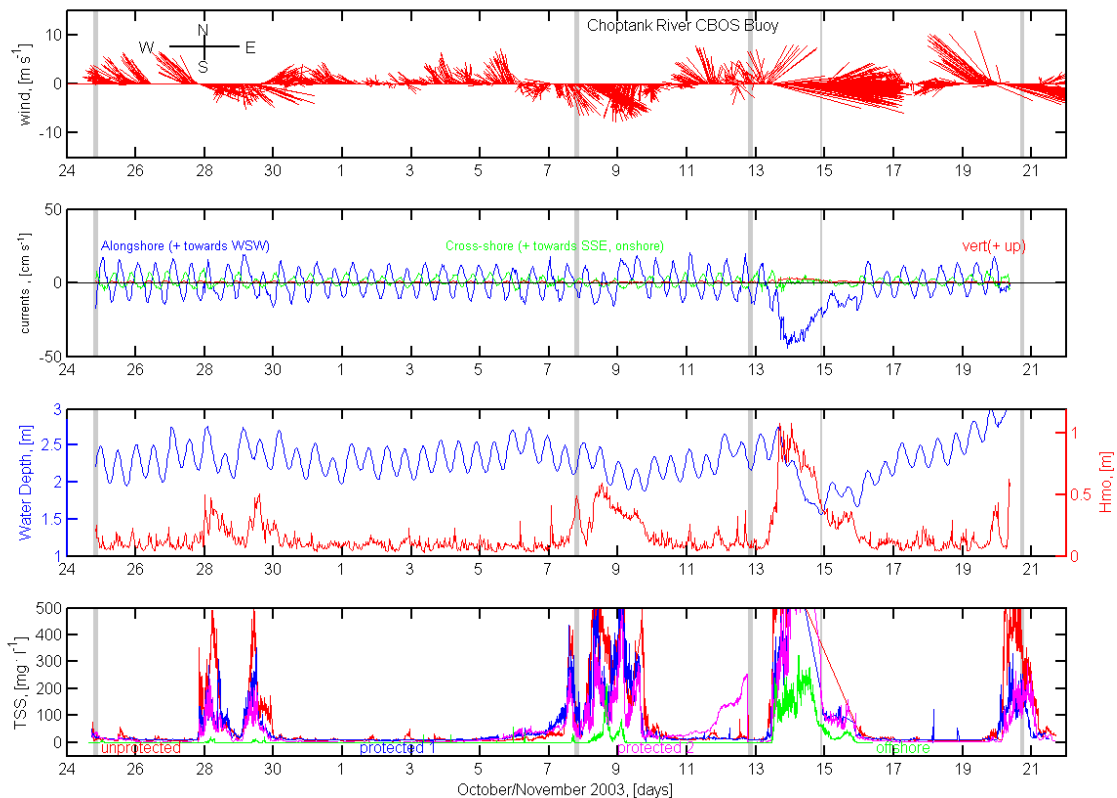


**Figure 24. Time series from moored sensors for the period of the 2003 Todds Point deployment. All variables and panels same as in Figure 23. Light gray vertical lines show times of boat surveys.**

Summary TSS statistics from all calibrated turbidity sensors from the 2002 and 2003 deployments are presented in Table 7. There are thousands of observations for each sensor, such

that these statistics are very robust. The statistics are presented in terms of the mean, median, and several measures of the percentage distribution rather than mean and variance because the TSS distributions were so obviously non-normal. This is completely consistent with the observation above that the records are event dominated, with relatively few very large values during wave events and low values otherwise; thus, the median TSS values are much lower than the mean values and the distributions are highly skewed. Comparing between years, 2003 TSS levels were somewhat lower than 2002 levels, most likely reflecting somewhat lower wave energy during the 2003 deployment. Comparing the nearshore to the offshore records, the nearshore TSS levels were much greater than the offshore by any measure; note in particular that the median offshore TSS was below detection and 85% of values were  $< 10 \text{ mg l}^{-1}$  in 2003, while the nearshore median TSS values were all  $> 10 \text{ mg l}^{-1}$ , with mean values  $> 50 \text{ mg l}^{-1}$ . Comparing alongshore in the nearshore zone, unprotected side TSS values were usually slightly larger than the protected side TSS values. The most significant difference between the two sensors deployed along the protected shoreline in 2003 was that site closer to the unprotected, eroding shoreline had fewer very low values and more intermediate values. During large events there was little alongshore difference between TSS at the nearshore sites.

**Table 7. Summary statistics from all deployed turbidity sensors for both deployment periods, calibrated using numerous in-situ bottle samples.**

Location	Year	TSS [ $\text{mg} \cdot \text{l}^{-1}$ ]		TSS Stats (%)			
		Mean	Median	% < 10	% >10 & <100	% > 100	% > 400
Unprotected	2002	105	43	32.7	25.7	35.1	6.5
Protected1	2002	91	31	25.9	39.6	28.8	5.7
Offshore	2002	15	7	57.2	41.6	1.2	0
Unprotected	2003	66	13	35.4	43.2	16.6	4.8
Protected1	2003	51	14	23.3	60.2	14.5	2
Protected2	2003	54	11	48.5	32.4	16.5	2.6
Offshore	2003	13	0	84.8	9.7	5.5	0

More detailed examinations of several of the events in 2002 and 2003 are presented in the following. All events and all maps are not presented here.

The first large event of the 2002 deployment is presented in Figure 25, which shows the data from the moored sensors for a 3-day period starting on October 29, 2002. There are several interesting aspects of this record. Winds were moderate to strong and dominantly from the north throughout the period. Moderately high waves persisted as well, ranging between approximately 0.2-0.5 m wave height. Nearshore TSS was the highest observed during both deployments, even though the waves were not the highest observed. Note that the TSS values are clipped at  $500 \text{ mg l}^{-1}$ , the upper limit of the OBS sensor during this deployment. A less sensitive setting was chosen for the 2003 deployment. The reasons for the very large TSS values with only moderately high wave heights are not completely clear. It may be that the direction of the waves favored shore erosion more during this event; the unprotected shore faces almost due North, such that the waves were directed straight onshore. This explanation is favored by the seeming

dependence of protected side TSS on the direction of the alongshore tidal current. Positive currents (towards the WSW) near the beginning of the event appear to have advected high TSS around the corner quite effectively. In fact, the protected side TSS values were often higher than the unprotected side TSS values during the early part of the event. When current directions changed towards the ENE near the end of the event, protected TSS dropped below unprotected TSS. The offshore site was only marginally affected by this event, indicating that the waves were not sufficient to cause significant resuspension at 2 m depth. TSS levels were quite low before the event, and they decreased rapidly as the forcing decreased in strength.

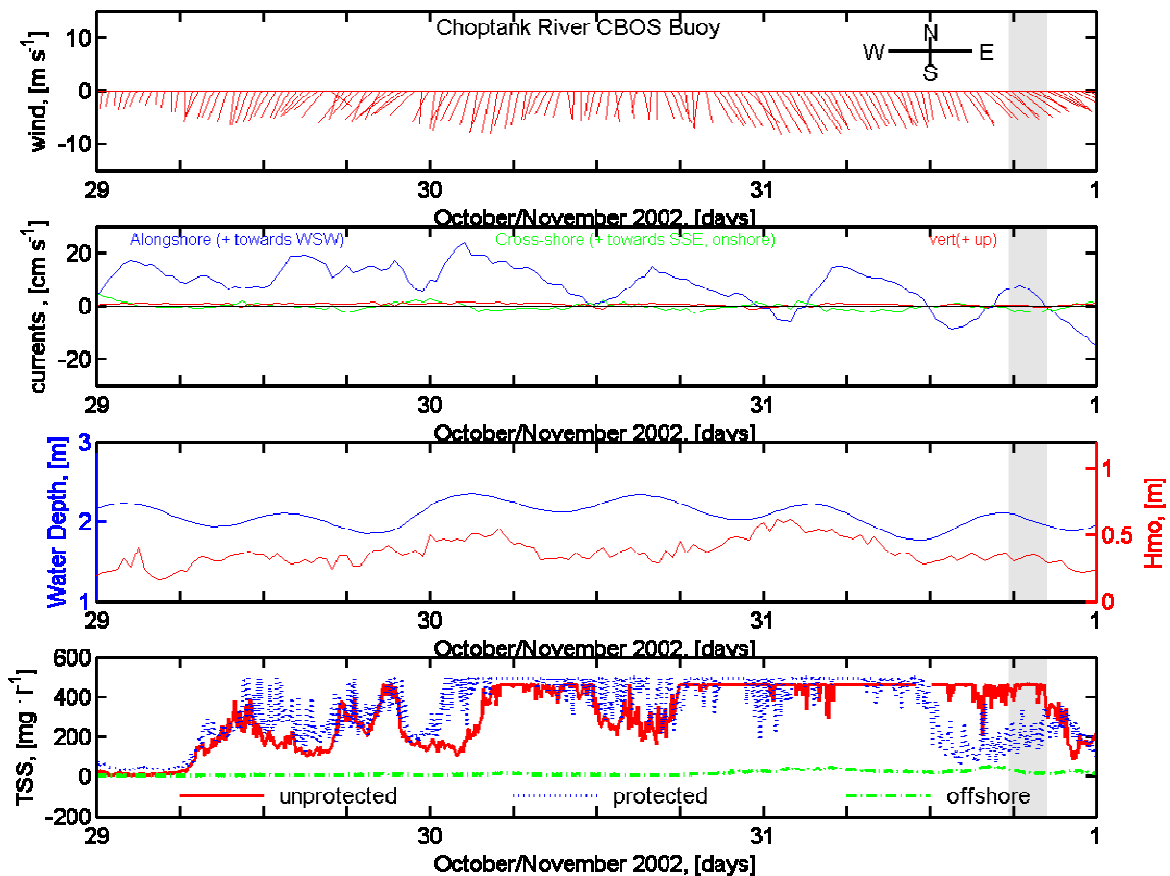


**Figure 25. Time series from moored sensors at Todds Point from Oct 29 – Nov 1, 2002. All variables and panels same as in Figure 23. Light gray vertical bar shows period of boat survey in Figure 26.**

An interpolated map of the horizontal distribution of TSS from the boat survey late on Oct. 31 near the end of the event is shown in Figure 26. Very high TSS levels are confined within approximately 150 m of the shoreline, and are either dispersed offshore or deposited locally further out. TSS on the unprotected side is higher than on the protected side, in agreement with the time series in Figure 25, but high TSS levels extend well down the protected shoreline.

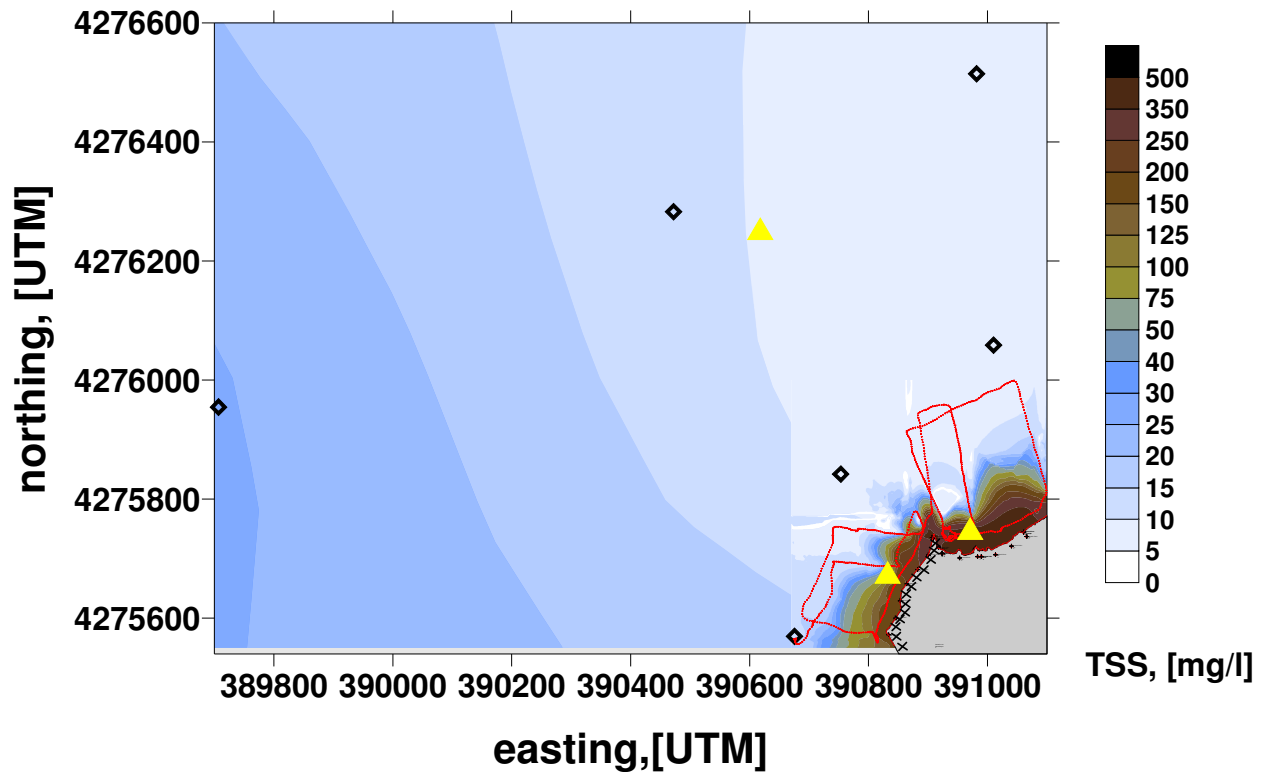


**Figure 26. Interpolated map of the horizontal distribution of TSS from the boat survey late on Oct. 31, 2002. Yellow triangles show locations of the moored sensors. Red line shows the kayak track, and black diamonds show CTD profile locations from the 25 ft. vessel.**

The second large event of the 2002 deployment is presented in Figure 27, which shows the data from the moored sensors for a 3-day period starting on November 6, 2002. While the same qualitative correspondence between winds, waves, and nearshore turbidity as in the first event is apparent, there are some notable differences. In particular, wave heights are approximately twice those in the earlier event, but nearshore TSS levels are not quite as high. This is most probably because the wave heights were measured offshore, where shoreline orientation is not as important as in the nearshore. Because the winds (and presumably the waves) were from the WNW, they attacked the unprotected shoreline at much more of an oblique angle than in the first event. This seems like the most probably explanation of the lower response. It is also notable that the offshore TSS response was the largest of this deployment. This is probably because tidal heights were falling while waves were still large, leading to large wave-induced velocities near bottom at the offshore location and significant resuspension.

The boat survey on Nov. 8 occurred during maximum ebb tide approximately one day after the event, just after a minor event of unknown cause recorded in the nearshore sensors. An

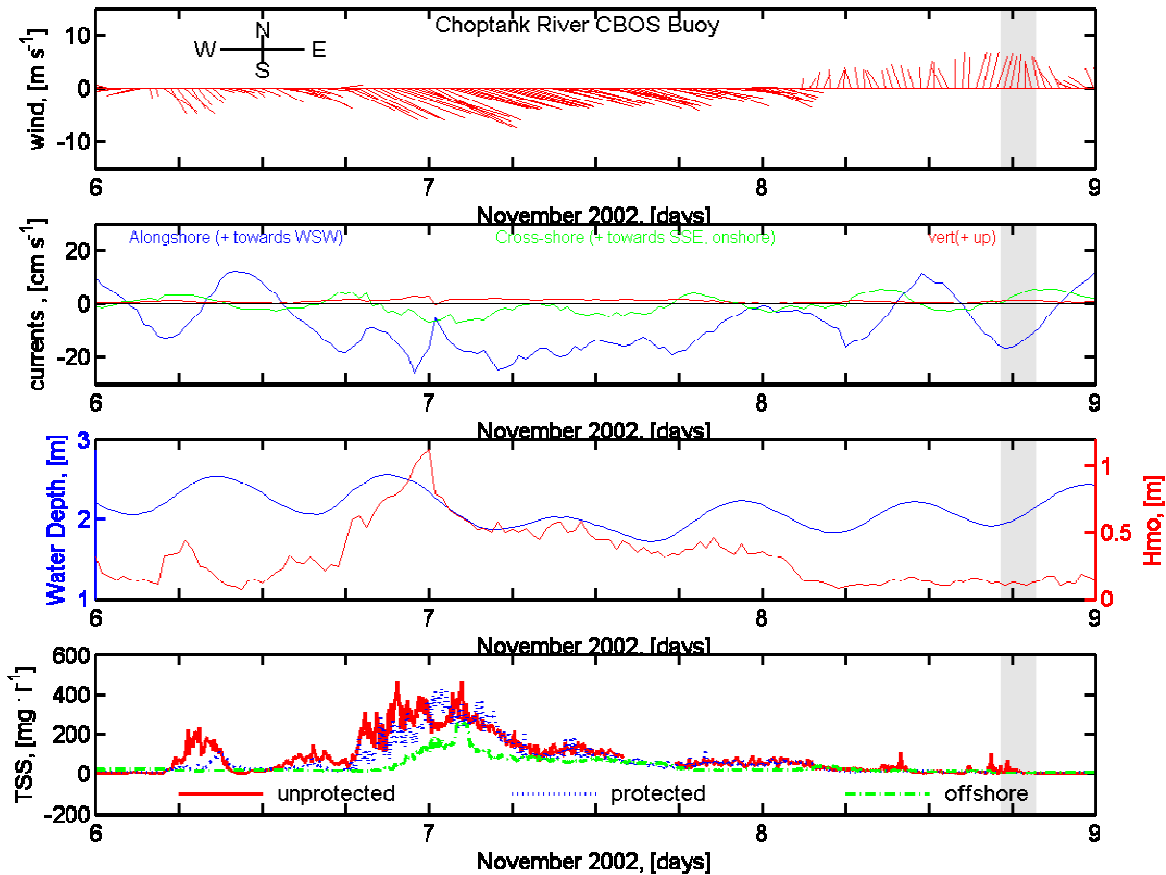


**Figure 27. Time series from moored sensors at Todds Point from Nov 6 – 9, 2002. All variables and panels same as in Figure 23. Light gray vertical bar shows period of boat survey in Figure 28.**

interpolated map of the horizontal distribution of TSS from this boat survey is shown in Figure 28. Overall levels of TSS are quite low, but small patches of slightly elevated TSS are being advected away from Todds Point by the ebb currents. There is no evidence of the large event on the previous day. A similar rapid return to background conditions is apparent in the interpolated TSS map from the boat survey of Nov. 14, which is not shown. Background conditions during a very calm period on Nov. 21 are shown in Figure 28, in which all TSS levels are  $< 10 \text{ mg l}^{-1}$  except for the very near vicinity of the junction between protected and unprotected shorelines. This location almost always exhibited slightly elevated TSS and was visibly more turbid.

The most interesting and contrasting event of the 2003 deployment is presented in Figure 29, which shows the three day period starting on Nov. 13, 2003. During this period strong westerly winds led to sustained 1 m high waves at the offshore site, but they also led to very low tide levels as water was forced out of the Bay. TSS levels at the nearshore sites rose rapidly until the falling tide left the sensors behind, exposing the bottom and moving the waterline offshore (Figure 15). The low water levels and large waves led to significant resuspension of bottom

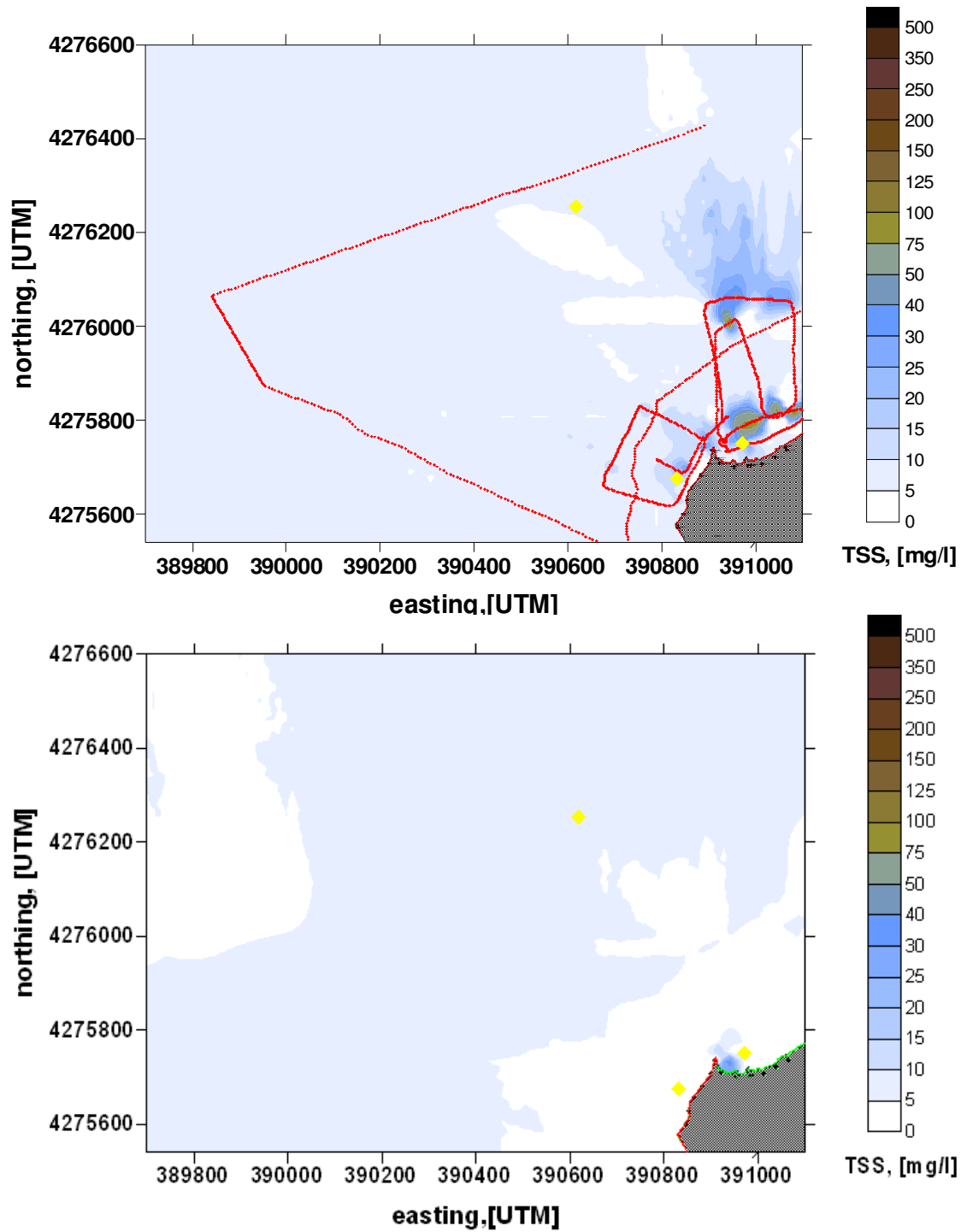


**Figure 28. Interpolated maps of TSS from boat surveys of Nov. 8 (top) and 21 (bottom), 2002. For timing of these surveys relative to events, see Figure 23.**

sediments at the offshore location, probably supplemented by offshore dispersion of suspended sediments from the nearshore. Clearly, however, little or no shore erosion itself occurred during the period of low tides.

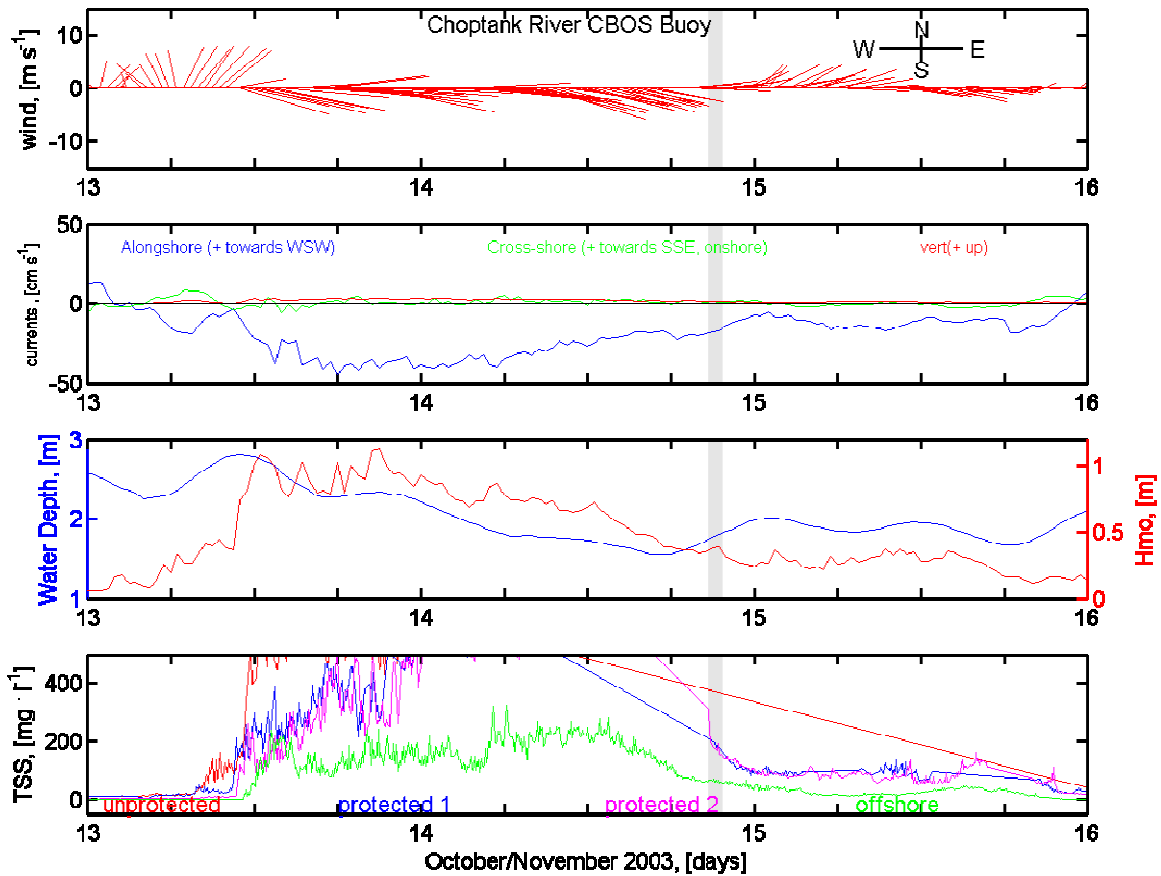


**Figure 29** Time series from moored sensors at Todds Point from Nov 13-16, 2003. All variables and panels same as in Figure 24. Light gray vertical bar shows time of photograph in Figure 15. There was insufficient water for a boat survey.

A boat survey on Nov. 12, 2003 (not shown), just prior to the event of Figure 29, closely resembles the survey of Nov. 21, 2002 (Figure 28). TSS levels throughout the domain were  $< 10 \text{ mg l}^{-1}$ , except for the very near vicinity of the boundary between the unprotected and protected shorelines. The boat survey of Nov. 21, 2003 (Figure 30) occurred after the offshore moored sensors had ceased recording, such that direct measurements of waves, currents, and tidal height are not available. However, the time series of nearshore TSS levels (Figure 24) indicate that the boat survey occurred near the height of an event. Evidence of significantly elevated TSS is apparent approximately 400 m offshore, although the highest concentrations occur within 200 m of shore. This survey was carried out closest to the peak of any of the events sampled in 2002 or 2003, and it shows the maximum observed extent of nearshore turbidity.

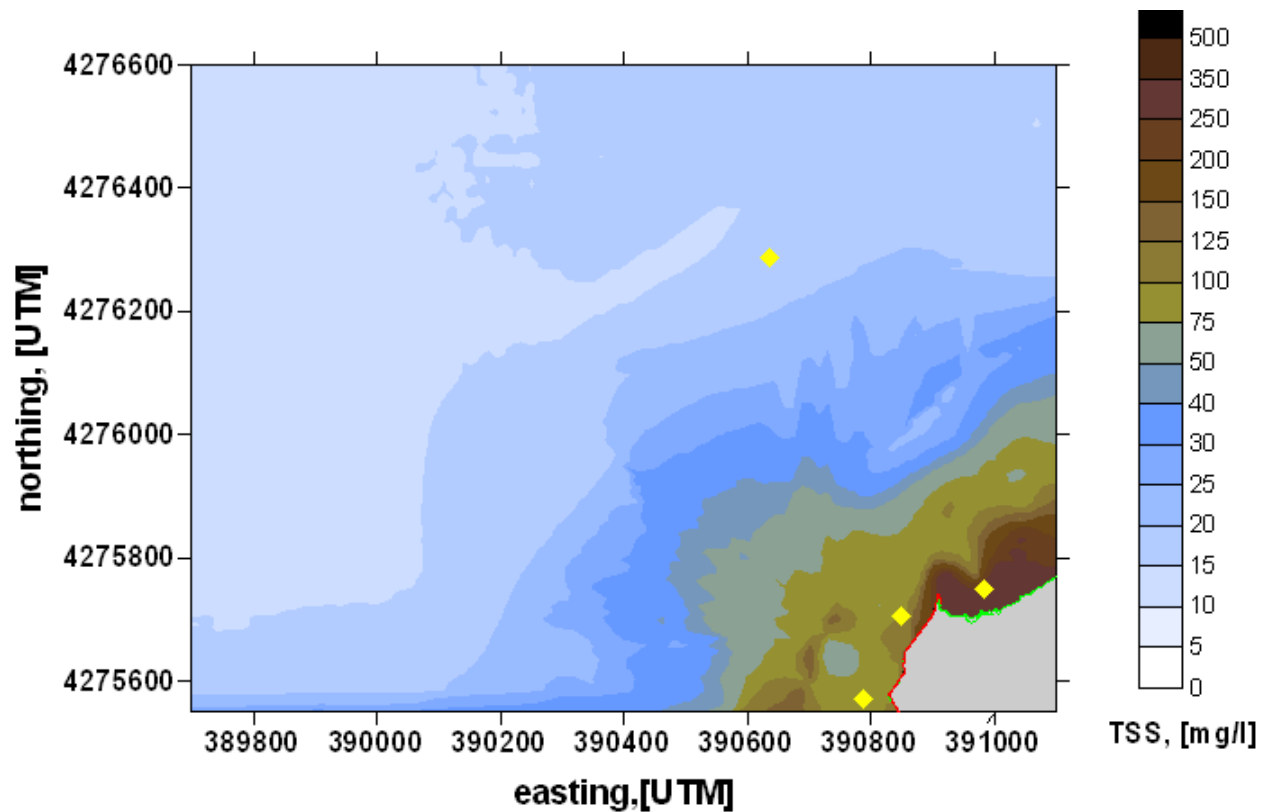


**Figure 30. Interpolated map of TSS from the boat survey of Nov. 21, 2003. For timing of this survey relative to an event, see Figure 24.**

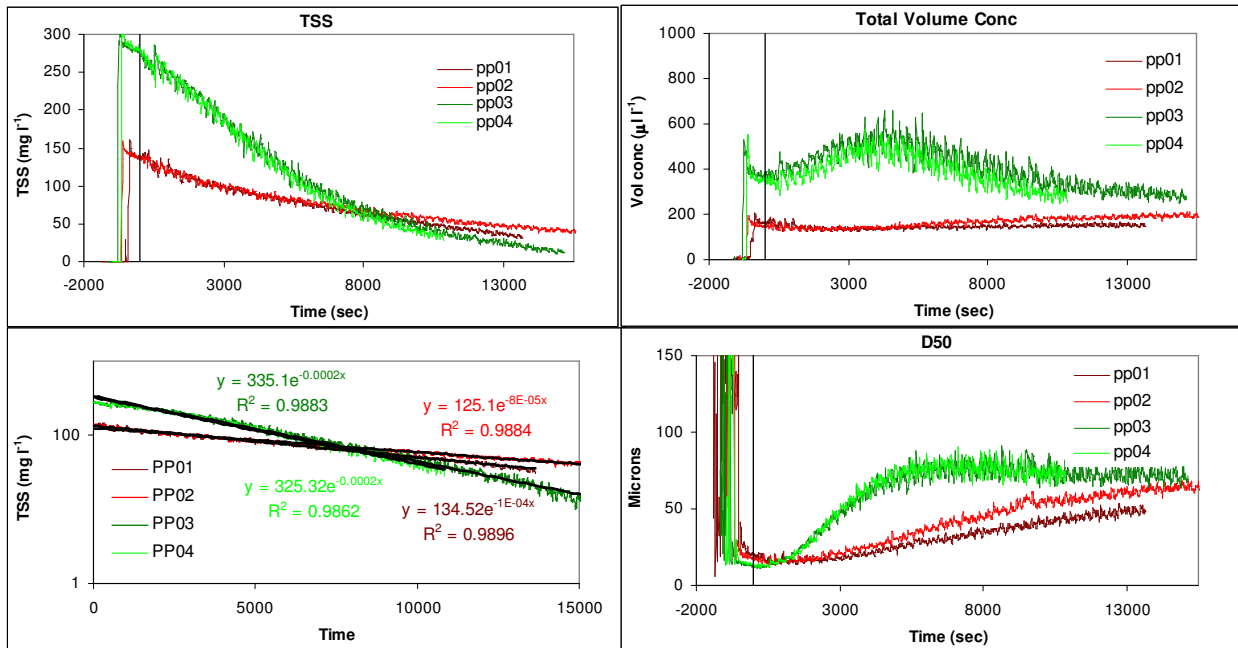
### Settling Velocity Experiments

Table 8 summarizes the primary results of the laboratory settling experiments. Results are reported for 8 sediment/soil sample settling experiments with different characteristics and initial concentrations. The total mass of sediment added to the 1000 l tank does not convert directly into the initial concentration because the sand fraction settled out prior to beginning the settling experiment, leaving behind the slower settling sediments that are of most interest here. The concentration at the beginning of the settling experiment is reported as the initial concentration. The settling velocities were derived by fitting Equation 2 to the observed time series of TSS (see below for more discussion). The fits to Equation 2 were generally quite good, yielding  $r^2$  values  $> 0.97$  in 6/8 cases and  $> 0.67$  in 2/8 cases (UP01 and UP02).

Data on mass concentration from the OBS sensors (both raw and fit to Equation 2), volume concentration from the LISST, and median particle size from the LISST are presented in Figure 31. Four of the 8 experiments summarized in Table 8 are presented as an example of the behaviors observed. Results from the remaining experiments were slightly more complex, but retain many of the features shown in Figure 31.

**Table 8. Summary of results of laboratory settling experiments. Bank samples from exposed unprotected eroding bank, UP samples from unprotected side bottom sediments near sensor pole, PP samples from protected side bottom sediments near sensor pole.**

ID	Settling Speed (mm s <sup>-1</sup> )	Mass Sediment Added (g)	Initial Conc. (mg l <sup>-1</sup> )	Sand %	Silt %	Clay %
Bank2	0.2	300	234	6	65	29
Bank3	0.1	300	236			
UP01	0.08	300	36	84	11	5
UP02	0.04	300	34			
PP01	0.1	300	138	35	51	14
PP02	0.08	300	137			
PP03	0.2	600	277			
PP04	0.2	600	276			



**Figure 31. Time series of mass concentration (top left), volume concentration (top right), mass concentration after beginning the settling experiment with exponential decay fits (bottom left), and median suspended particle diameter (bottom right) from the Protected Pole laboratory settling experiments.**

Given the behavior shown, it is remarkable that the Equation 2 gives such a good fit to the data. Equation 2 assumes that the settling velocity of the material in suspension remains constant over the period of observation, which yields a good fit to the mass concentration data. However, it is apparent from the LISST data that the actual processes occurring during settling are much more complicated. All experiments, but especially the high initial concentration ones, indicate active flocculation as the total volume concentration and median diameter of the particles increases

while the mass concentration is decreasing. After approximately 1 hour in the high concentration experiments, the volume concentration, mass concentration, and median diameter all begin to decrease due to settling, though at different rates. Thus, it appears that simultaneous flocculation and settling yield the same mass behavior as a constant mass settling velocity in this case.

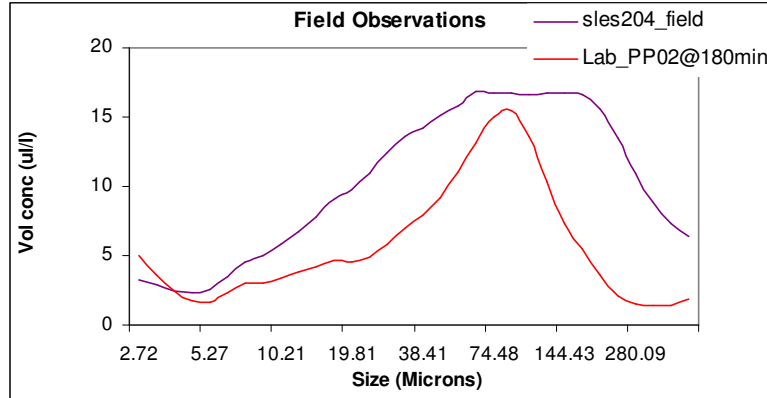


**Figure 32. – LISST size distributions from field observations at Todds Point. (blue line) for comparison to laboratory observations from experiments on samples from site PP02. The field and laboratory concentrations were both approximately 130 mg l<sup>-1</sup>.**

A comparison of limited LISST data from one survey in the field to data from a laboratory experiment with similar initial concentration (both close to 130 mg l<sup>-1</sup>) indicates that the laboratory experiments may offer a reasonable representation of behavior in the field (Figure 32). In both cases, the floc size distributions peak in approximately the same size range, which is nominally that of a fine sand. In both cases, however, there were no sand particles in suspension, such that the observed particles must be flocs of finer silts and clays. This is very similar to the findings of Sanford et al. (2005) when examining flocculated suspended sediments in upper Chesapeake Bay.

Figure 33 shows that the variability in derived settling speeds from the laboratory experiments may be at least partially explained by concentration-dependent flocculation processes. Many previous studies have reported that equilibrium floc size (hence settling velocity) increases with increasing suspended sediment mass concentration, because collisions between particles that lead to flocculation are much more frequent at higher concentrations. The data from the laboratory experiments support this behavior. In addition, previous authors have indicated that the increase in size/settling speed is not very significant below concentrations of order 10<sup>2</sup> mg l<sup>-1</sup>, which is also consistent with the data shown (though not with the simple linear fit). Finally, the general range of settling speeds in Table 8 and Figure 33 corresponds to a sediment particle settling 1 m in approximately 1.5 – 5.5 hours, which is consistent with the time scale of clearing following the erosion events described in the previous section.

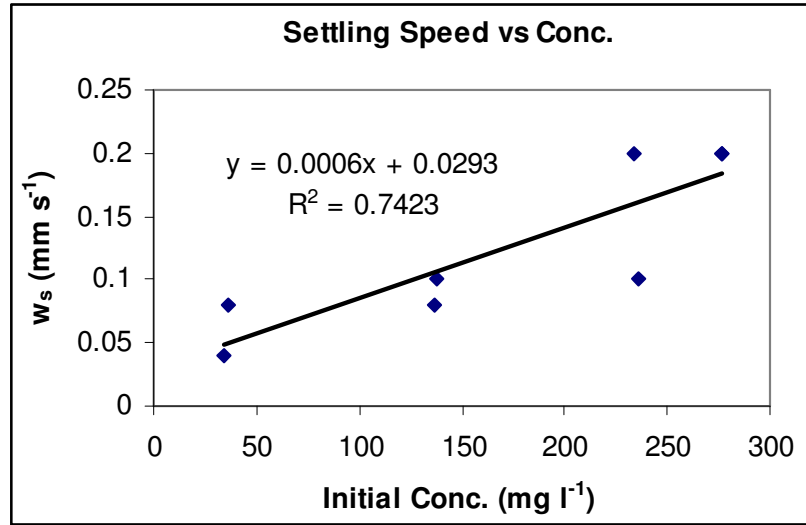


**Figure 33. Initial concentration vs. derived settling speed from the laboratory experiments summarized in Table 8.**

### Exploratory Modeling

The results of fitting Equation 4 (visually) to the observed offshore bathymetric profiles at Todds Point are presented in Figure 34. The agreement is remarkable, given that the majority of bathymetric profiles upon which Equation 3 is based are from sandy beaches. Even more remarkable is the fact that the derived fitting constant  $A = 0.022 \text{ m}^{1/3}$  is in the middle of the range of values expected for sediment sizes near the silt-sand boundary (Figure 1 in Dean (1991)). There are several important aspects of this figure. First, it appears that all three bathymetric profiles have a large bar between approximately 350-650 m offshore, where elevations are up to 0.5 m higher than expected from Equation 4. There are at least two possible reasons for this bar. It may be that the sand fraction present in the eroding shoreline is transported offshore until it can no longer be moved by the prevailing waves and currents, which would indicate that this offshore bar should be significantly sandier than the sediments further inshore. It may also be that the depth of this feature, approximately 1.5 m below mean tide, is the effective wave base for typical wave conditions at the site, preventing further downward erosion of the nearshore as the shoreline keeps retreating. Another important feature of these profiles is that the protected shoreline profile matches up with the eroding shoreline profiles if it is translated offshore 63 m, which is equal to the estimated retreat of the unprotected shoreline at  $2.5 \text{ m y}^{-1}$  over the 25 years since the protected shoreline was hardened. This implies that the nearshore zone off the protected shoreline continued to deepen at the same rate as the nearshore profile off the unprotected shoreline, even though shoreline retreat itself was stopped. If this hypothesis is correct, the nearshore zone off the protected shoreline will continue to deepen as the unprotected shoreline retreats, at least until it reaches the 1.5 m depth of the offshore bar.

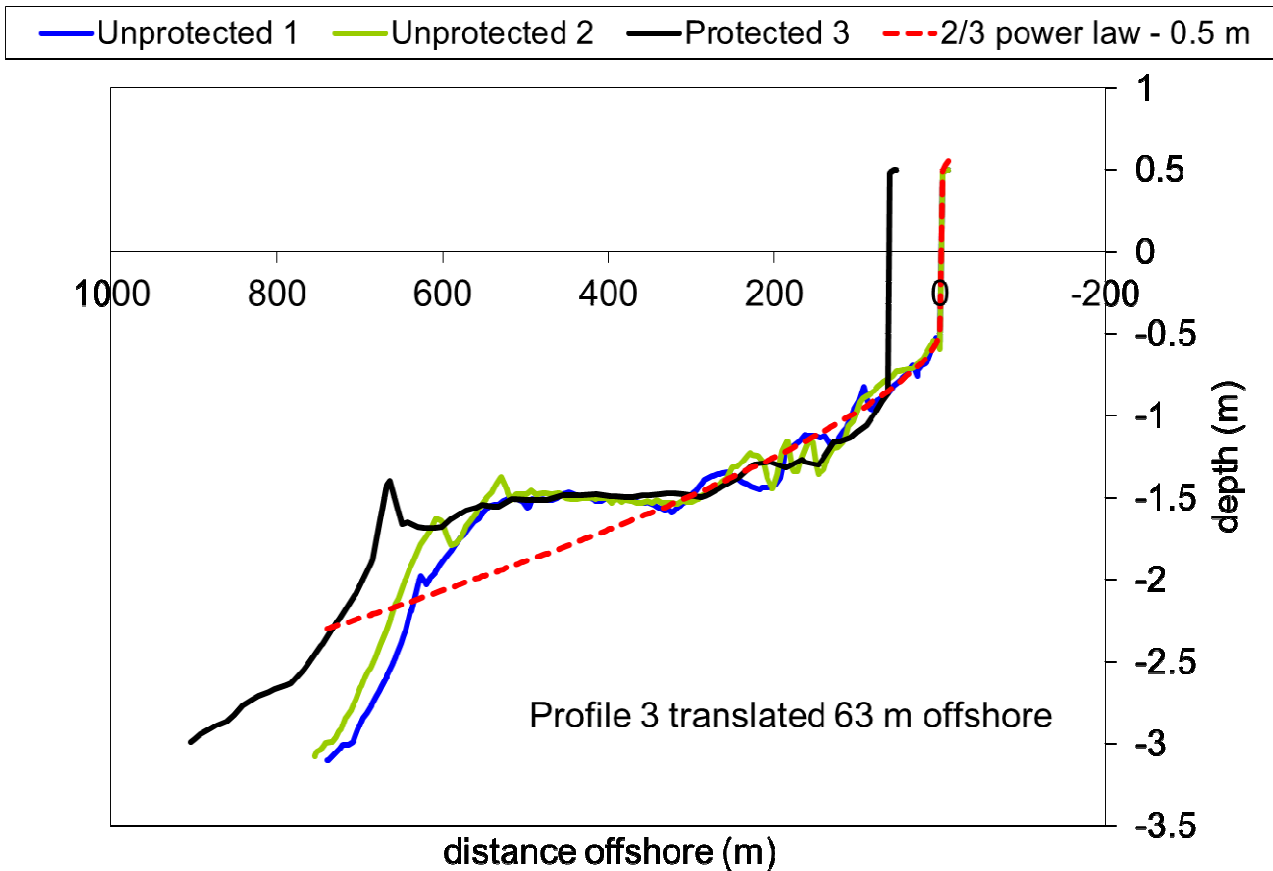


**Figure 34. Bathymetry along cross-sections off the unprotected and protected shorelines at Todds Pt. relative to mean tide, compared to equilibrium 2/3 power law model with 0.5 m offset.**

Figure 35 shows the results of applying the two shoreline erosion models described in the methods to elevation data and wave height estimates from October 2002 through November 2003. The elevation and wave height estimates were both low-pass filtered with a 24 hr. cutoff to remove astronomical tides, leaving only the wind-forced storm tides and corresponding wave estimates. For purposes of discussion, we refer to the model derived from Miller and Dean (2004) and described by Equations 6, 7, and 10 as Model A. We refer to the model derived from Wilcock et al. (1998) and described by Equations 11, 13, and 15 as Model B.

The essential difference between these models is that Model A assumes that surf zone processes control shoreline movement, while Model B assumes that direct erosion of the shoreface controls the rate of shoreline retreat. It is apparent from Figure 35 that either model can be calibrated (through adjustment of a single constant  $k$  or  $K$ ) to yield the observed 2.5 m shoreline retreat over the 402 days between shoreline surveys. It is further apparent that both models attribute most erosion to large events that correspond to episodes of high waves, such that the relatively stormy fall and winter seasons (the first 130 days and the last 70 days) experience the most rapid erosion and the relatively calm spring and summer periods

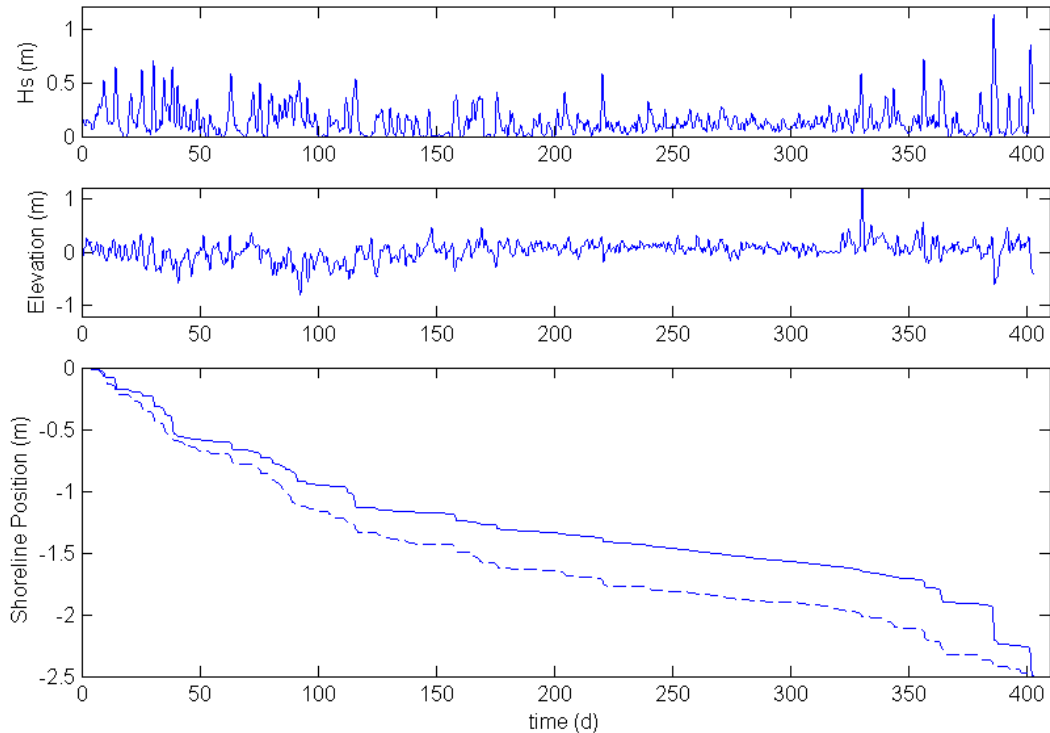


**Figure 35. Time series of lowpass filtered (24 hr cutoff) model-predicted wave height (top), observed tidal height (middle) and predicted shoreline retreat (lower panel) from Model A (solid line) and Model B (dashed line). The models were calibrated to give the observed total erosion over the period of the simulation.**

(the middle 200 days) experience much slower rates of erosion. However, which events are most important varies significantly between the models. Model A attributes more erosion to fewer events, probably because of its more stringent requirements on sea level in order to have an active surf zone. Model B distributes less erosion between more and slightly different events.

An alternative view of the model predictions relative to data is presented in Figure 36. Here we assume that direct shoreline erosion is the most important cause of nearshore turbidity events. We compare observed nearshore turbidity to the predictions of both models, forced with unfiltered measured waves and measured tidal height from the periods of the deployments only. Here the differences between the two models are more apparent. Model A predicts shoreline erosion during some of the observed events, but completely misses the magnitude of approximately half of the events. Model B is a much more consistent predictor of nearshore turbidity, hence (presumably) the timing of shoreline erosion events. Note that both models predict that erosion ceases during the very low tide event on day 22 in 2003 (see figure 23.). An equally intriguing feature of the models is the prediction that the passage of Hurricane Isabel (see very high tidal heights on approximately day 330 in Figure 35) resulted in relatively little shoreline erosion. This makes sense because a closer examination of the data during Isabel (not shown) reveals that winds were all offshore during the period of maximum tidal elevation at Todds Point. Thus, tidal heights were very high but there were few waves, resulting in little erosion.

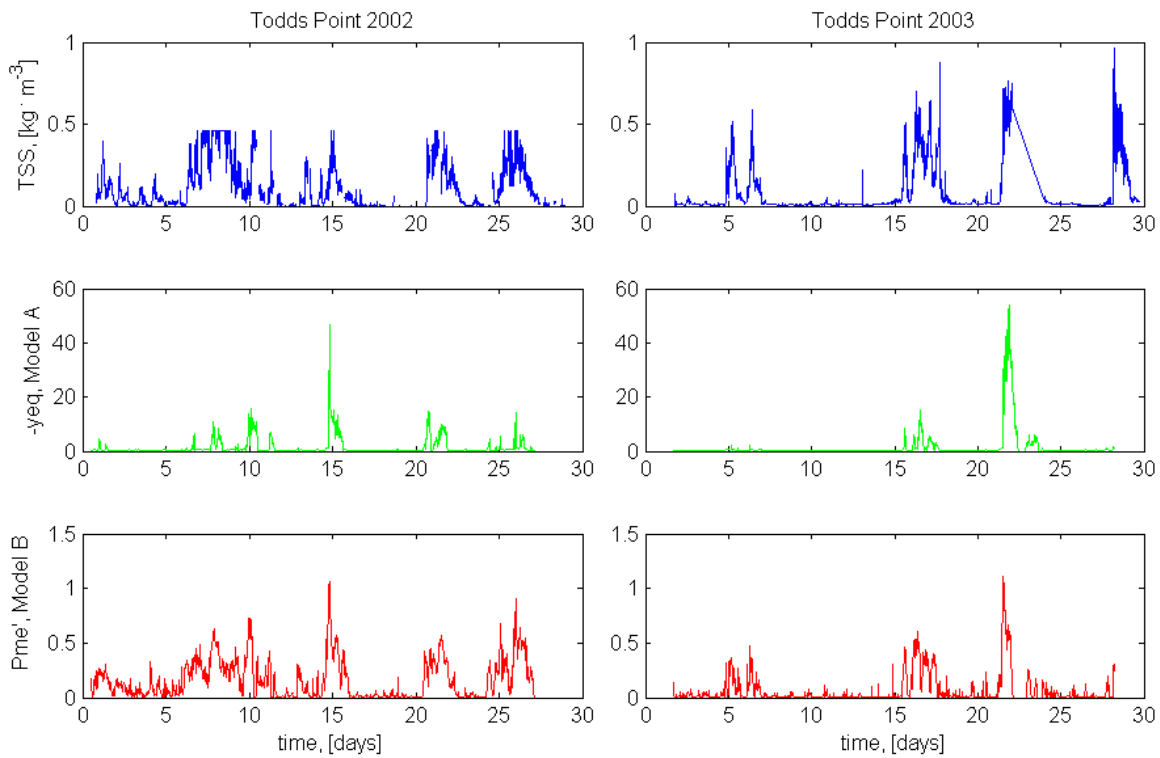


**Figure 36. Observed nearshore TSS time series from the unprotected side sensor (top panel), predicted shoreline erosion impulse from Model A (middle panel) and predicted shoreline erosion impulse from Model B (lower panel). The left column predictions are forced by observed wave and tidal height observations in 2002 (Figure 23), while the right column predictions are forced by observations from 2003 (Figure 24).**

## **ACKNOWLEDGEMENTS**

Partial funding for this study was provided by the Environmental Protection Agency - Chesapeake Bay Program to the Maryland Department of Natural Resources. The authors gratefully acknowledge the able field assistance provided by Richard Ortt and Steve VanRyswick of the Maryland Geological Survey, and Steven Suttles and Patrick Dickhudt of the University of Maryland Center for Environmental Science. Historic shore erosion rate determinations were provided by E. Lamere Hennessee and Katherine Offerman of the Maryland Geological Survey. We also gratefully acknowledge the cooperation of Mr. Robert Spedden, who allowed us land access to his shoreline and told us about the history of the property.

## RERERENCES

- Anders, F.J. and Byrnes, M.R., 1991. Accuracy of shoreline change rates as determined from maps and aerial photographs. *Shore and Beach*(January): 17-26.
- Berman, M.R., Berquist, H., Dewing, S., Hershner, C.H., Rudnicky, T., Barbosa, A., Woods, H., Schatt, D.E., Weiss, D., and H. Rea, 2003. Dorchester County, Maryland Shoreline Situation Report, Comprehensive Coastal Inventory Program, Virginia Institute of Marine Science, College of William and Mary, Gloucester Point, Virginia, 23062
- Berman, M.R., Berquist, H., Killeen, S., Nunez, K., Rudnicky, T., Schatt, D.E., Weiss, D. and K. Reay, 2005. Talbot County, Maryland - Shoreline Situation Report, Comprehensive Coastal Inventory Program, Virginia Institute of Marine Science, College of William and Mary, Gloucester Point, Virginia, 23062
- Cleaves, E. T., Edwards, J., and Glaser, J., 1968, *Geologic Map of Maryland: Maryland Geological Survey.*
- Crawford, S.M. and Sanford, L.P., 2001. Boundary shear velocities and fluxes in the MEERC experimental ecosystems. *Marine Ecology Progress Series*, 210: 1-12.
- Danforth, W.W. and Thieler, E.R., 1992. *Digital Shoreline Analysis System (DSAS) User's Guide*, Version 1.0. 92-355, U.S. Geological Survey.
- Hicks, S. D. and L. E. Hickman, Jr., 1988, United States sea level variations trough 1986: *Shore and Beach* 56: 3-7.
- Hill, J. M., Wikel, G., Wells, D. V., Hennessee, E. L., and Halka, J. P., 2003, *Shoreline Erosion as a Source of Sediments and Nutrients: Chesapeake Bay, Maryland: Maryland Geological Survey*, 03-02.
- Kearney, M. S., and Ward, L. G., 1986, Accretion rates in brackish marshes of a Chesapeake Bay estuarine tributary: *Geo-Marine Letters*, v. 6, p. 41-49.
- Kearney, M. S., and Stevenson, J. C., 1991, Island Land Loss and Marsh Vertical Accretion Rate Evidence for Historical Sea-Level Changes in Chesapeake Bay: *Journal of Coastal Research*, v. 12, no. 4, p. 403-415.
- Kearney, M. S., Stevenson, J. C., and Ward, L. G., 1994, Spatial and temporal changes in marsh vertical accretion rates at Monie Bay: Implications for sea-level rise.: *Journal of Coastal Research*, v. 10, p. 1010-1020.
- Kearney, M. S., 1996, Sea-level Change during the Last Thousand Years in Chesapeake Bay: *Journal of Coastal Research* 12(4): 977-983.
- Kerhin, R. T., J. P. Halka, et al. 1988. The surficial sediments of Chesapeake Bay, Maryland: Physical characteristics and sediment budget, Maryland Geological Survey, Report of Investigations No. 48, 160 pp.
- Kerhin, R.T, Hennessee, E.L, Isoldi, J.J., and Gast, R.A., 1994, 1997, *Shoreline Changes: Maryland Geological Survey, Baltimore, Md.*, 99 maps.
- Lin, W., Sanford, L.P. and Suttles, S.E., 2002a. Wave measurement and modeling in Chesapeake Bay. *Continental Shelf Research*, 22(18-19): 2673-2686.
- Lin, W., Sanford, L.P., Suttles, S.E. and Valigura, R.A., 2002b. Drag Coefficients with Fetch Limited Wind Waves. *Journal of Physical Oceanography*, 32(11): 3058-3074.
- Maa, J. P.-Y., L. P. Sanford, and J.P. Halka, 1998, Sediment resuspension characteristics in Baltimore Harbor, Maryland: *Marine Geology* 146: 137-145.

- Maryland Geological Survey, 2000, Shoreline Changes, Tilghman Quadrangle, MD. Baltimore, MD. 1:20,000, 1 sheet. [http://www.mgs.md.gov/coastal/maps/slmapdf/TILGH\\_PF.pdf](http://www.mgs.md.gov/coastal/maps/slmapdf/TILGH_PF.pdf)
- Maryland Geological Survey, 2001, Shoreline Changes, Hudson Quadrangle, MD. Baltimore, MD. 1:20,000, 1 sheet. [http://www.mgs.md.gov/coastal/maps/slmapdf/HUDSO\\_PF.pdf](http://www.mgs.md.gov/coastal/maps/slmapdf/HUDSO_PF.pdf)
- Owen, M.W., 1976. Determination of the settling velocities of cohesive muds. Hydraulics Research, Wallingford, 24 pp.
- Owens, J. P. and C. S. Denny, 1986a, Geologic Map of Dorchester County, Maryland Geological Survey, scale 1:62,500.
- Owens, J. P., and C. S. Denny, 1986b, Geologic Map of Talbot County: Maryland Geological Survey, scale 1:62,500.
- Sanford, L. P., 1994, Wave forced erosion of bottom sediments in upper Chesapeake Bay: *Estuaries* 17(1B): 148-165.
- Sanford, L. and J. P. Halka, 1993, Assessing the paradigm of mutually exclusive erosion and deposition of mud, with examples from upper Chesapeake Bay: *Marine Geology* 114: 37-57.
- Sanford, L.P., Suttles, S.E. and Halka, J.P., 2001. Reconsidering the physics of the Chesapeake Bay Estuarine Turbidity Maximum. *Estuaries*: 24(5): 655-669.
- Sanford, L.P. et al., 2005. Variability of suspended particle concentrations, sizes and settling velocities in the Chesapeake Bay turbidity maximum. In: I.G. Droppo, G.G. Leppard, P. Liss and T. Milligan (Editors), *Flocculation in Natural and Engineered Environmental Systems*. CRC Press, LLC, Boca Raton, Florida, pp. 211-236.
- Stevenson, J. C., Kearney, M. S., and Pendleton, E. C., 1985, Sedimentation and erosion in a Chesapeake Bay brackish marsh system: *Marine Geology*, v. 67, p. 213-235.
- Shalowitz, A.L., 1964. *Shore and Sea Boundaries*. 10-1, U.S. Government Printing Office, Washington, D.C.
- U.S. Army Corps of Engineers, 2002, *Coastal Engineering Manual*: U.S. Army Corps of Engineers, 1110-2-1100.
- US Army Corps of Engineers, 1990, *Chesapeake Bay Shoreline Erosion Study, Feasibility Report*.
- Wilcock, P.R., Miller, D.S., Shea, R.H. and Kerkin, R.T., 1998. Frequency of effective wave activity and the recession of coastal bluffs: Calvert Cliffs, Maryland. *Journal of Coastal Research*, 14(1): 256-268.

## **APPENDIX**

### Site Descriptions for Bank Sample Locations

**Site ID:**

**Site name:** Cook Point North

**Location:** East side Cook Point, at the North end.

UTM Zone 18 NAD83, m	Northing	Easting
Actual	4275950	0388257

**Date:** 10/01/02

**Time:** 12:09 EDT

**Described by:** J Halka

**Shoreline type (e.g., marsh, bluff, beach):** bluff

**Extent (length) of reach (ft):** 1,000 feet

**Bank elevation (ft):** 2.5 feet

**Land use/cover along reach:** Grasses and low

Shrubs backed by forest

Location of bank sample.



**Site description:**

Vertical clay bank topped with grasses and low shrubs with some small trees. Bank is 2.8 feet high, with 4 foot wide horizontal shelf in front at current water level, then another 2.9 foot vertical drop to an underwater shelf. Underwater shelf is fairly hard and has some sand accumulating in low points.

**Reach description:**

Reach is about 1000 feet long, grading to a lower elevation bank topped with all grasses to the north, and at the same elevation to a point to the south. Reach to south is topped with more trees.

Cook Point, North looking to north.



**Samples:**

ID	Type*	Location**
#1	BD, GS	Middle of bluff

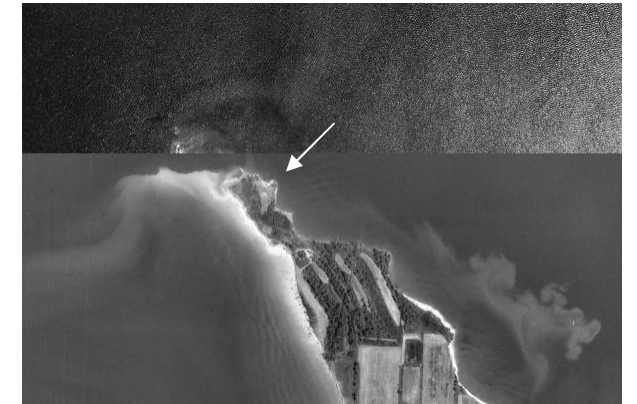
\***Type** = bulk density (BD); grain size (GS); trace metal (TM)

\*\***Location** = show on stratigraphic section

**Photos:**

Date	Time EDT	Subject
10/01/02	12:22	Bluff at sample, location
10/01/02	12:25	Bluff to north

**Plan view**



Air photo taken 1998

**Site ID:**

**Site name:** Cook Point South

**Location:** East side Cook Point, just to north of Cook Point Cove

UTM Zone 18 NAD83, m	Northing	Easting
Actual	4275138	0389187

**Date:** 10/01/02

**Time:** 12:43DT

**Described by:** J Halka

**Shoreline type (e.g., marsh, bluff, beach):** bluff

**Extent (length) of reach (ft):** 2000 feet

**Bank elevation (ft):** 3 feet

**Land use/cover along reach:** Narrow strip of grasses and low shrubs backed by forest

Cook Point South at sampling location.



**Site description:**

Vertical clay bank topped with grasses and low shrubs with forest behind. Bank is 3.2 feet high. A narrow sand beach occurs on either side of the point and widens to both the north and the south.

**Reach description:**

Reach is about 2000 feet long. Forest cover is more notable to both north and south. Beach is larger to both north and south.

**Plants:**

Species	Percent

Looking to north of sampling location.



**Samples:**

ID	Type*	Location**
#2	BD, GS	Middle of bluff

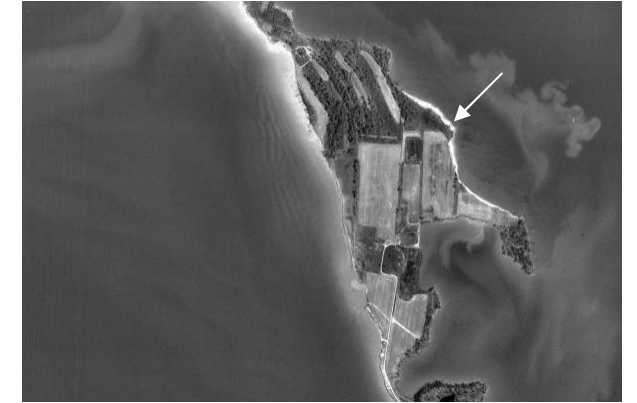
\***Type** = bulk density (BD); grain size (GS); trace metal (TM)

\*\***Location** = show on stratigraphic section

**Photos:**

Date	Time EDT	Subject
10/01/02	12:50	Bluff at sample, location
10/01/02	12:51	Bluff to north

**Plan view**



Air photo taken 1998

**Site ID:**  
**Site name:** Deep Neck Point  
**Location:** East side Broad Creek

UTM Zone 18 NAD83, m	Northing	Easting
Actual	4287985	0392498

**Date:** 10/01/02  
**Time:** 14:10 EDT  
**Described by:** J Halka  
**Shoreline type (e.g., marsh, bluff, beach):** Bluff  
**Extent (length) of reach (ft):** 800 feet  
**Bank elevation (ft):** 3-4 feet  
**Land use/cover along reach:**  
 Corn field  
 Bank sample location at Deep Neck Point.



**Site description:** 3.4 foot high clay bluff, probably Kent Island formation. Very hard and difficult to sample. Upper layer (below plow zone) is about 2 feet thick, darker color and somewhat softer than the lower lighter colored layer which is about 1 foot thick. The lower layer is too hard to drive core into, and sample is collected by driving a screwdriver into the bank and bagging a sample. Offshore this material is being rewatered and is very soft, supports SAV.

**Reach description:**  
 Reach is about 800 feet long. To south the property is reveted in front of home and outbuildings. To north new home construction and revetment in place.

Looking to north of sampling location



**Samples:**

ID	Type*	Location**
#1	BD, GS	Upper section of bluff in darker layer
#3	BD, GS	Lower section of bluff in lighter colored layer
#2	GS	Core collected underwater about 40 feet offshore, in rewatered bank material

\***Type** = bulk density (BD); grain size (GS); trace metal (TM)  
 \*\***Location** = show on stratigraphic section

**Photos:**

Date	Time EDT	Subject
10/01/02	14:14	Bluff at sample location
10/01/02	14:15	Bank to North
10/01/02	14:15	Bank to South



Photo taken in 1994

**Site ID:**

**Site name:** Tilghman Island East #1

**Location:** South of Dogwood Harbor

UTM Zone 18 NAD83, m	Northing	Easting
Actual	4284096	0384312

**Date:** 10/01/02

**Time:** 14:50 EDT

**Described by:** J Halka

**Shoreline type (e.g., marsh, bluff, beach):** Marsh

**Extent (length) of reach (ft):** 300 feet

**Bank elevation (ft):**

**Land use/cover along reach:**

Forested and low scrub

**Site description:** Small marsh at the level of the water on this day. Approximately 2.5 foot erosional scarp underwater. Entire bank face is organic peaty marsh material, as is the offshore bay bottom.

**Reach description:**

Reach is about 300 feet long. To north more homes and shoreline is reveted. To south forested shoreline is fronted by numerous fallen trees making access impossible.

**Plants:**

Species	Percent

**Samples:**

ID	Type*	Location**
#1	BD, GS	Peaty material from eroding marsh face

\*Type = bulk density (BD); grain size (GS); trace metal (TM)

\*\*Location = show on stratigraphic section

**Photos: None**

Date	Time EDT	Subject

**Plan view**



Photo taken in 1994

**Site ID:**

**Site name:** Todds Point East

**Location:** Eastern end of Todds Point.

UTM Zone 18 NAD83, m	Northing	Easting
Actual	4275957	0391788

**Date:** 10/01/02

**Time:** 13:16 EDT

**Described by:** J Halka

**Shoreline type (e.g., marsh, bluff, beach):** Bluff

**Extent (length) of reach (ft):** 1,500 feet

**Bank elevation (ft):**

**Land use/cover along reach:** Grasses and low shrub backed by forest along most of reach, soy field behind grasses to west.

Looking to East of sampling location.



**Site description:**

Vertical bluff with natural vegetation on top. Bluff is about 3 feet high and composed of compacted silts and clays. Narrow beach at base of bluff. Upper 1.5 feet is a light grey color, lower 1.5 feet is a darker grey color. No apparent textural difference between the layers.

**Reach description:**

Small beach at base of bluff widens to the west. To the east about 1000 feet the shoreline is protected by revetment. About 500 feet offshore the remains of an apparent former shoreline revetment occur in about 4-5 feet of water depth (Could have been a breakwater rather than revetment).

Looking to west of sampling location.



**Samples:**

ID	Type*	Location**
#1	GS, BD	Taken in upper light grey layer
#2	GS, BD	Taken in lower dark grey layer

\***Type** = bulk density (BD); grain size (GS); trace metal (TM)

\*\***Location** = show on stratigraphic section

**Photos:**

Date	Time EDT	Subject
10/01/02	13:30	View to east of site
10/01/02	13:31	Bank face at sample site
10/01/02	13:31	View to west of site. Soy field behind first group of trees.

**Plan view**



Air photo taken 1994

Bank at sampling location.



**Site ID:**

**Site name:** Todds Point

**Location:** South shore of the mouth of Choptank River

UTM Zone 18 NAD83, m	Northing	Easting
Site U1	4275713	390954
Site U6	4275745	391061

**Date:** 9/30/02

**Time:** 1:00 – 4:00 PM (EDT)

**Described by:** DVW

**Shoreline type (e.g., marsh, bluff, beach):** bluff with narrow beach

**Extent (length) of reach (ft):** ~1000 ft

**Bank elevation (ft):** 2-4 ft

**Land use/cover along reach:** Agriculture; corn fields; farm house



Photo: Todds Pt. looking east along unprotected core shoreline.

**Site description:**

Site U1: Located at west end of unprotected reach, near vertical bluff with grasses on top. Bluff is 3.2 feet high. Upper 1.6 feet composed of med. gray to blue gray silty-clays, weathering to brownish yellow. The upper section is undercut forming a shallow cave, ~2-3 feet deep. The lower portion of bluff is compacted clay which is more resistant to erosion, thus forming a shelf which extends 10-15 feet out from bluff and is exposed at low tide..

Site U6: Located at east end of reach where bluff is ~ 2 ft high, face consisting of med gray to gray sandy silty clay. Sandy beach in front of bluffs along this end of reach.

**Reach description:** Todds Pt. on south side of mouth of Choptank River; reach includes small cove facing north, extending east 1000 ft from Todds Pt. and west facing rip-rapped reach west of Pt. Unprotected shore dominated by low bluffs, sparse natural vegetation. Shoreline moderately convoluted. Active agriculture field (corn) within 10 feet of edge of bluffs.

**Samples:**

ID	Type*	Location**
U1-A	BD, GS	Top of bluff face
U1-B	BD, GS	Bottom of bluff, on clayey shelf
U6-A	BD, GS	Middle of bluff face

\***Type** = bulk density (BD); grain size (GS); trace metal (TM)

\*\***Location** = show on stratigraphic section

**Photos:**

Date	Time EDT	Subject
9/30/02	12:22	Todds pt, duck blind
9/30/02	12:23	Cove. looking east
9/30/02	1:33	Collecting bluff sample at site U2
9/30/02	1:46	Bluff at U2, showing undercut bank
9/30/02	1:47	Close-up of undercut bank
9/30/02	2:01	Site U6- bank sample
9/30/02	4:30	Detail of bluff along core
9/30/02	4:31	Todds pt., duck blind
9/30/02	4:31	Todds pt cove, looking east at low
9/30/02	4:32	Rip rap reach at Todds Pt, looking south
9/30/02	4:32	Rip rap reach, looking north toward Todds Pt.

**Plan view**



Air photo taken 1994



Photo: Close up of undercut bank at Site U6

**Site ID:**

**Site name:** Tilghman Island East #2

**Location:** Upper Bar Neck Point

UTM Zone 18 NAD83, m	Northing	Easting
Actual	4282351	0384879

**Date:** 10/01/02

**Time:** 15:30 EDT

**Described by:** J Halka

**Shoreline type (e.g., marsh, bluff, beach):** Bluff

**Extent (length) of reach (ft):** 100 feet

**Bank elevation (ft):** 5 feet

**Land use/cover along reach:**

Corn field

**Site description:** .5 foot high vertical bluff fronted by very narrow beach of fine sand. Material is firm compacted clays and silts. Offshore small embayment is floored by rewatered material that has become very soft.

**Reach description:**

Reach is about 100 feet long. To north forest backs the shoreline and access is difficult. Erosion rate seems lower than at site. To south and east the small point is protected by revetment.

**Plants:**

Species	Percent

**Samples:**

ID	Type*	Location**
#2	BD, GS	Middle of the eroding bluff

\***Type** = bulk density (BD); grain size (GS); trace metal (TM)

\*\***Location** = show on stratigraphic section

**Photos:** None, bank face in shadow.

Date	Time EDT	Subject

**Plan view**



Photo taken in 1994

**Site map:**



**Martin O'Malley**, Governor  
**Anthony G. Brown**, Lt. Governor  
**Joseph P. Gill**, Secretary  
**Frank W. Dawson III**, Deputy Secretary

---

The Maryland Department of Natural Resources (DNR) seeks to balance the preservation and enhancement of the living and physical resources of the state with prudent extraction and utilization policies that benefit the citizens of Maryland. This publication provides information that will increase your understanding of how DNR strives to reach that goal through the earth science assessments conducted by the Maryland Geological Survey.

#### MARYLAND DEPARTMENT OF NATURAL RESOURCES

Resource Assessment Service  
Tawes State Office Building  
580 Taylor Avenue  
Annapolis, Maryland 21401  
Toll free in Maryland: 1-877-620-8DNR  
Out of State call: 1-410-260-8021  
TTY users: Call via the Maryland Relay  
[Internet Address: dnr.Maryland.gov](http://dnr.Maryland.gov)

#### MARYLAND GEOLOGICAL SURVEY

2300 St. Paul Street  
Baltimore, Maryland 21218  
Telephone Contact Information: 410-554-5500  
[Internet Address: mgs.md.gov](http://mgs.md.gov)

DNR Publication Number 12-632013-650  
June 2013

*The facilities and services of the Maryland Department of Natural Resources are available to all without regard to race, color, religion, sex, sexual orientation, age, national origin or physical or mental disability.  
This document is available in alternative format upon request from a qualified individual with a disability.*